July 1988
LU TP 88-13

How to Discriminate between High-p_T Physics Monte Carlos

Torbjörn Sjöstrand
Department of Theoretical Physics,
University of Lund, Sölvegatan 14A,
S-223 62 Lund, Sweden

Abstract:
All currently available QCD-inspired models/Monte Carlos for the event structure in high-p_T physics are described. Included is information on hard interactions, initial and final state radiation, structure functions, beam jets and fragmentation. Results from a number of comparative Monte Carlo runs are presented, which help to illuminate how the physics content in Monte Carlos may be tested. Special emphasis is put on the partial observability of coherence effects in initial state radiation, and on differences in the jet structure of high-p_T events.

1. Introduction

Hadronic physics is complex enough that still today, 15 years after the arrival of QCD on the stage, any absolute predictive power is rather limited. This is particularly apparent if one is given the task of describing the complete event structure in hadron-hadron collisions. In order to make any headway at all, it is necessary to subdivide (by brute force) the problem into a few more or less disjoint components.

The standard electroweak model and perturbative QCD can be used to calculate lowest order hard scattering matrix elements. When combined with Q^2-dependent structure functions, a very successful basic framework is obtained for the p_T spectrum and angular distribution of hard jets (modulo K factors and jet definition uncertainties).

The logical continuation of the perturbative approach would be the calculation of higher order diagrams. Unfortunately, whereas people have become quite proficient in calculating Born graphs, the calculation of loop graphs to the same order has not kept pace. The matrix element alternative is therefore not particularly attractive for high energy applications. The standard choice is instead to supplement the lowest order matrix element with initial and final state parton shower evolution. This is an approximate approach, but it can be used to represent arbitrarily complicated parton configurations, of the kind that seems to be required experimentally.

The perturbative QCD description is in terms of coloured partons, but the experimentally observable entities are colour singlet hadrons, leptons and photons. The intervening stages of fragmentation and decay have, so far, proved too difficult for exact QCD calculations. Instead various, loosely QCD-motivated, fragmentation models are used.

Finally, the partons scattered from the incoming hadrons leave behind remnants, which experimentally show up as the low-p_T beam jets. This is probably the point where the physical modelling is most uncertain, so the spread between different approaches is considerable.

In order to include sufficiently realistic scenarios for each of the components mentioned above, and to put it all together into a detailed modelling of the complete event structure, only the Monte Carlo computer program approach is flexible and powerful enough. The programs that will be discussed here are ISAJET [1], PYTHIA [2], HERWIG [3], COJETS/WIZJET [4], FRITIOF [5], EUROJET [6] and FIELDAJET [7]. To the best of my knowledge, these are all the existing programs that set out to describe events involving hard interactions. In addition, a number of programs exist for the study of low-p_T events only; these will not be covered here. In one of these, DTUJET [8], hard interactions have recently been included, but so far without initial or final state radiation, so it is not yet a realistic alternative for high-p_T physics.

Obviously all the programs have been constructed to describe the same observed physics - with some time dependence in what is known and has therefore been used to constrain aspects of the models. In general, this leads to large similarities in the predictions of the models, even when the physics input is rather disparate. In this paper I have therefore concentrated on isolating areas where discrepancies between models can still be found, so that experimental data could be used to constrain the models. The results are reasonably encouraging. For initial and final state parton showers, it seems feasible to set nontrivial constraints on the lower cutoff of the shower evolution, and also to isolate some signals for coherence effects (the expected reduction of gluon emission by destructive interference [9,10,11]). The study of multijet states would constrain several aspects of the models. Differences between quark and gluon jet fragmentation are already observed experimentally [12], and further studies would here be helpful. Overall particle composition is generally comparable between models, but the composition in specific regions of phase space may show large differences. Finally, string effects can and should be looked for.

Given the state of our ignorance, it is not reasonable to expect any program to agree perfectly with data. If disagreements are sufficiently large, or appear in crucial distributions, it is still reason enough to distrust the physics framework used in the afflicted programs. In this sense, comparisons between Monte Carlos and data can tell us not only the relative merits of the programs, but also of the underlying physics.

2. Program and Physics Survey

In this section, the Monte Carlo programs will be compared with respect to their physics contents. The following programs are discussed:

- ISAJET by Paige and Protopopescu [1], version 6.00, with roughly 15 k lines of code.

- PYTHIA by Bengtsson and Sjöstrand [2], version 4.8, with 7 k lines (plus another 6 k in JETSET 6.3 [13], which is used for fragmentation/decay).

- HERWIG by Marchesini and Webber [3], version 2.2, with 6 k lines.

- COJETS/WIZJET by Odorico [4], each program with 5 k lines, much of which is common.

- FRITIOF by Andersson, Gustafson, Nilsson-Almqvist, Sjögren and Stenlund [5], with 3 k lines (plus the use of PYTHIA for the selection of hard interactions and JETSET for fragmentation/decay, see above).

- EUROJET by Ali, van Eijk and Pietarinen [6], with 11 k lines.

- FIELDAJET by Field and coauthors [7], size unknown. Actually FIELDAJET is not a publicly available program, in contrast to the others listed here, and so not much can be said about it.

2.1. Hard Interactions

Perturbative matrix element calculations for parton interactions have been completed up to order α_s^3, i.e. including 2→2 and 2→3 Born terms and 2→2 one loop corrections. The 2→4 Born terms are also available, but none of the loop corrections to the same order. Based on the experience from e^+e^- annihilation, where full second order corrections are available, it is known that the inclusion of higher orders is needed to describe the event structure, and that second order is not enough (the four-jet rate is underestimated, e.g.) [14]. Further, multijet structures are expected to become increasingly important with increasing (transverse) energy, so at current collider energies the situation should be even worse than it was at PETRA/PEP.

This shortfall is the reason why most programs only contain Born graphs, and include the emergence of a multijet structure by parton shower evolution. The exception is EUROJET, where 2→2, 2→3 and 2→4 Born terms are included, and no showers. In the future it is hoped to include 2→n graphs, with n≥5, either in the form of exact matrix elements or in an approximate form designed to reproduce the correct pole behaviour. This offers an interesting alternative approach to parton showers, but leaves open the potentially dangerous issues of K factors and consistent phase space cutoffs.

Since the matrix element approach is geared towards the emission of hard radiation, and parton showers towards soft or collinear one, in the best of possible worlds the two approaches should be married, but issues of doublecounting makes this nontrivial [15]. Information from loop calculations could also be used in an approximate fashion, to deduce K factors, relevant Q^2 scales or modified threshold behaviours (e.g. for $gg \to c\bar{c}$ [16]).

Essentially all programs covered here contain the standard 2-jet cross-sections and the production of a single W or Z, where switches can be set to select the process of interest (in the COJETS/WIZJET pair, the two tasks are separated, with W/Z production in WIZJET). The ISAJET and PYTHIA programs in addition contain just about all other 2→1 and 2→2 standard model Born graphs, such as arbitrary pairs of γ, W, Z and jets, and various modes for Higgs production. ISAJET also contains supersymmetric pair production (squarks, gluinos, photinos, winos, zinos), and PYTHIA some other non-standard particles (H^+, Z', a horizontal gauge boson). EUROJET includes several of the standard model 2→2 graphs, and is the only program to cover leptoquark production. HERWIG contains some Higgs production channels, but generally HERWIG, COJETS/WIZJET, FRITIOF and FIELDAJET are less versatile.

2.2. Structure Functions

In order to select the kinematics of a hard interaction, matrix elements have to be folded with the structure functions of the two incoming hadrons. Most frequently used in recent years have here been the parametrizations EHLQ sets 1 and 2 [17] and DO sets 1 and 2 [18]. Because of the initial state showering algorithms used in COJETS/WIZJET and FIELDAJET, these programs do not need Q^2-dependent structure functions, but instead use their own fixed Q^2 structure function sets.

With the continued accumulation of data, several new sets have recently appeared [19]. These are not available as parametrizations, however, but rather as very large data grids in x and Q^2. This makes them less appealing for inclusion in Monte Carlos. EUROJET contains an interface to the MRS sets, but this is rather an exception. An alternative is to provide a direct interface to an evolution program, where the data grids can be generated from user-defined fixed Q^2 structure functions. Thus the Tung program [20] is interfaced with PYTHIA.

2.3. Initial and Final State Radiation

In general, the subdivision of multiparton event production into initial state radiation, hard interaction and final state radiation is not gauge invariant. Exceptions do exist, however: in e^+e^- annihilation all QCD radiation is in the final state, and in hadron collider W/Z production (with the W/Z decaying leptonically) there is only initial state QCD radiation. Even in more complex situations, a pragmatical subdivision is feasible. The hard interaction is then the 2→2 subprocess with largest Q^2, initial state radiation has its poles along the incoming hard partons and final state radiation has its poles along the scattered partons. As mentioned above, this approach is most uncertain for hard emission away from the collinear regions.

Initial and final state parton showers may both be seen as treelike structures, where successive branchings of the types $q \to qg$, $g \to gg$ and $g \to q\bar{q}$ leads to the emergence of complicated multiparton states. The branching probabilities are given by the well-known Altarelli-Parisi equations. In this approximation, the branching rules are independent of the nature of the hard interaction, which makes for a convenient universal description.

Despite the usage of the same basic branching rules, the structure of an initial and a final shower is rather different. The latter cascade is timelike: all partons have mass-squared $m^2 \geq 0$. The parton that emerges from the hard interaction has the largest mass, and then successively branches into partons with smaller and smaller masses and energies, until eventually all partons end up on mass shell (modulo confinement effects). The initial state shower, on the other hand, is spacelike: the sequence of partons leading up from the shower initiator to the parton entering the hard interaction is characterized by $Q^2 = -m^2 > 0$; only the side branches (not leading up to the hard interaction) are timelike. As the shower evolves, the energy is again

split between more and more partons.

The Monte Carlo treatment of initial state showers contains a number of problems. If the evolution is traced forwards, starting at the low Q^2 shower initiator, it is beforehand not known which daughter parton in a branching is spacelike and which timelike, and neither is the upper Q^2 limit of the evolution known. In the normal process of overcoming these problems, a large fraction of the showers generated are rejected, which makes for low efficiency. Thus, FIELDAJET, with forward evolution, is orders of magnitude slower than any other program on the market. Also COJETS/WIZJET is based on forward evolution, but with a sophisticated pretabulation machinery, which cuts generation time to a feasible level.

The alternative is backwards evolution, where the hard interaction is taken as starting point, and the shower is traced "backwards in time" towards the original shower initiator [21]. None of the conceptual or practical problems above then appears, although some computer time is lost by the need to evaluate structure functions at each branching. Backwards evolution is the strategy used in PYTHIA, ISAJET and HERWIG, with some local variations. In a slightly different formulation, it has also been used in FIELDAJET [22].

In recent years, the study of coherence effects have helped pin down some of the details of parton shower evolution. Particularly important is the destructive interference in the soft gluon emission probability for colour connected partons. This destructive interference can be correctly accounted for, in final state showers, by requiring the emission angle in subsequent branchings to be decreasing [10]. Final state coherence is included in HERWIG and PYTHIA, but absent in ISAJET, COJETS/WIZJET and FIELDAJET. Unfortunately, it is very difficult to find experimental signals for coherence effects; so far no evidence exists either way. (The observation of "string effects" in e^+e^- annihilation is sometimes quoted as evidence for coherence, but that is probably too simplistic a view [14].) The issue is further complicated by the wide range of non-coherent algorithms in use. Just one example: coherence effects are often claimed to reduce the rate of parton multiplicity increase with increasing energy, but actually the detailed kinematics of the non-coherent algorithm used in ISAJET makes the rate of increase at current energies slower than that in the coherent algorithm of HERWIG.

Coherence phenomena are significantly more complicated in initial state radiation. With the notation of Fig. 1, kinematics alone gives the requirements $z_1Q_1^2 < Q_3^2$, $z_3Q_3^2 < Q_5^2$, etc, i.e. the Q_i^2 need not even be strictly ordered. This is the region allowed in COJETS/WIZJET. A first constraint, coming from a study of leading collinear singularities, is that the Q_i^2 actually should be ordered: $Q_1^2 < Q_3^2 < Q_5^2$ [9]. This constraint is used in PYTHIA and ISAJET. In the latest year, studies of leading soft singularities have given the further constraint that transverse momenta of emitted timelike partons be ordered, i.e. $E_1\theta_2 < E_3\theta_4$ or $\theta_2 < z_1\theta_4$. For $z_1 \ll 1$ this reduces to the Q^2-ordering above, but for $1-z_1 \ll 1$ it gives $\theta_2 < \theta_4$, i.e. angular ordering [11,3]. In particular, note that a memory is retained of the shower initiator direction, even after many branchings - a rather counterintuitive result. So far, HERWIG is the only program to include this kind of coherence. The experimental confirmation of coherence effects is again not trivial, see section 3.1.

The approach to parton showers in FRITIOF is not based on the successive branching of one parton into two, but rather on the dual description, where repeatedly a colour dipole is split into two [23]. Here a quark is always associated with the end of a dipole, whereas a gluon, with its double colour charge, sits at the junction of two dipoles. This approach has the advantages of automatically including angular ordering constraints and of having a branching probability that only depends on the mass of a dipole. Even more impressive, no distinction need be made between initial and final state radiation, but both can be treated simultaneously and symmetrically. On the negative side, the dipole which is stretched between a scattered parton and the diquark target remnant can not be allowed to contain the full diquark energy, but only a fraction which is not known from first principles. Also, branchings of the type $g \to q\bar{q}$ are not yet included.

2.4. Fragmentation

Three main fragmentation schools exist: independent fragmentation (IF), string fragmentation (SF) and cluster fragmentation (CF) [14].

In IF, each jet is assumed to fragment independently of all other jets in the event. This basic assumption makes IF very easy to work with, and IF is also the most popular framework, being used in ISAJET, COJETS/WIZJET, EUROJET and FIELDAJET. Quark and gluon jet fragmentation properties can be specified

completely independently, although the two are usually assumed the same. IF is not Lorentz covariant, and neither does it explicitly conserve energy, momentum or flavour, so it can only be thought of as a rather crude approximation to any consistent underlying physics picture. In e^+e^- annihilation, IF is clearly disfavoured by data, but hadron physics is sufficiently more messy that no clear conclusions have been reached here.

In SF, the partons emerging from the hard interactions are assumed connected by strings, which may be thought of as a Lorentz covariant and causal description of colour flux tubes with a linear confinement force. Quarks and diquarks correspond to string endpoints whereas gluons, with their double colour charge, correspond to energy and momentum carrying kinks on these strings. A generally good description of e^+e^- annihilation data is obtained.

A specific problem is that the colour ordering of partons along the strings has to be specified before an event can be fragmented, and that this colour ordering seldom is unique. In PYTHIA, use is made of the observation that, on the amplitude level, all Feynman graphs can be associated with well defined colour flows. The squared amplitudes, i.e. the physical cross-sections, contain interference terms, but these are down in order by $1/N_c^2$ (where $N_c = 3$ is the number of colours) and can be neglected to first approximation. For a process like $qg \to qg$ two distinct colour topologies then remain, Fig. 2. In the parton shower stage added on top of the hard interaction, the colour flow again has to be traced, but this is straightforward so long as only the basic branchings $q \to qg$, $g \to gg$ and $g \to q\bar{q}$ are used.

In FRITIOF, which also is based on SF, it is rather assumed that there is never a net exchange of colours between two colliding hadrons - any exchange in hard interactions is neutralized by soft gluon interactions. This gives a picture of separate, diffractive type, colour singlet systems, with a unique colour flow. The price to be paid is that only processes of the type $qq \to qq$, $qg \to qg$ and $gg \to gg$, where q are valence quarks, may be considered. In particular, processes like W/Z production are not included.

In CF, finally, all gluons remaining at the end of the parton shower evolution are nonperturbatively split into $q\bar{q}$ pairs. These may be grouped into colour singlets, usually a q from one gluon branching and a $\bar{q}$ from an adjacent gluon. The singlets, clusters, are then allowed to decay isotropically, according to phase space. Like SF, this approach is Lorentz covariant, and explicitly conserves energy, momentum and flavour. Agreement with e^+e^- data is also

reasonable, although worse than with SF [14]. Clusters are used in HERWIG, and were also briefly used in FIELDAJET. Colour flow ambiguities are handled similarly in HERWIG as in PYTHIA; differences are restricted to the $1/N_c^2$ pieces.

2.5. Beam Jets

The simplest beam jet model is that in FIELDAJET, where the beam remnant is just considered as one further independently fragmenting quark jet. EUROJET is similar, but allows for leading baryon effects, and a by-hand "pedestal" of additional activity in hard jet events. In FRITIOF, one ordinary string piece is stretched out to the diquark beam remnant, while one valence quark is always pushed to central rapidities, and often over into the opposite hemisphere, by hard or soft gluon exchanges.

COJETS/WIZJET and HERWIG do not have any kind of continuity between high-p_T and low-p_T fragmentation phenomena, but rather use longitudinal phase space parametrizations for the low-p_T part, with multiplicity distributions and pedestal effects put in by hand. In the former twin programs, the longitudinal phase space is directly in terms of hadrons; in HERWIG clusters are used, à la the UA5 algorithm [24].

In ISAJET a cut Pomeron picture is used, with a variable number of Pomerons per event [25]. Each cut Pomeron corresponds to a back-to-back pair of low-p_T jets; this is slightly different to the normal DTU approach [26], where a cut Pomeron gives two chains, i.e. two pairs of back-to-back jets. Leading baryon effects and an increased number of Pomerons in high-p_T jet events are put in by hand. Fragmentation parameters are different from those assumed for high-p_T jets, and are explicitly energy dependent.

The most complex machinery is found in PYTHIA. In addition to the hardest interaction, it is assumed that further semihard interactions may occur in the same event, according to (truncated) perturbative QCD formulae [27]. For a fixed impact parameter, the number of interactions is distributed according to a Poissonian, but events with small impact parameters on the average contain more interactions, and are thereby also more likely to give rise to high-p_T jets. Ordinary strings are stretched out to the target remnants.

3. Program Comparisons

The previous section contained a fairly objective survey of what goes into the different programs. In this section, results of direct comparisons between programs will be presented. It has therefore not been feasible to devote equal time to all programs. FIELDAJET is not publicly available, and can be dropped without further ado. EUROJET has a rather distinct profile compared with the other programs, and is probably not competitive for general multijet structures. Its forte is instead the study of heavy flavour production, with lepton spectra, isolation criteria and background sources as main topics. All the other programs have been used, but some more than others.

Events generated with the different programs have been translated to a common format, so that subsequent analysis has been identical. For jet finding, a cluster routine à la the UA1 one has been used, assuming a grid of 100 bins between pseudorapidities $-5 < \eta < 5$ and 64 in azimuth ϕ, and requiring a transverse jet energy $> E_{Tmin}$ within a distance $((\Delta\eta)^2+(\Delta\phi)^2)^{1/2} = \Delta\omega < R$ around a jet initiator. An attempt has been made to present all comparisons in terms of physical observables, but not to take into account all the complexities of real life, which can only be assessed by a full detector simulation. This would also be necessary for a comparison with data, to find which program (if any) makes the "correct" predictions. The purpose of this study is then rather to discuss where physical differences should be looked for.

ISAJET and PYTHIA have been extensively compared within the framework of SSC studies [28]. These studies have been useful in finding programming errors, and have also helped underline how programs starting from disparate premises may in real life give very similar results. No corresponding comparisons between any of the other programs, or with data used to distinguish between different programs, are known to me.

3.1. Initial State Radiation

Initial state radiation is most conveniently studied in W (or Z) production, since the W transverse momentum spectrum is a direct probe of radiation effects. Experimentally, $\langle p_{TW}\rangle$ is 7 - 8 GeV [29], compared with the less than 1 GeV expected just from primordial k_T, i.e. without radiation.

The evolution of $\langle p_{TW}\rangle$ with CM energy is shown in Fig. 3. Note that ISAJET, PYTHIA and HERWIG have about the same slope, whereas the rate of increase in WIZJET is lower. This may be counterintuitive, since WIZJET is the only program without coherence constraints, and therefore should have the most extensive evolution. Kinematically, however, a larger number of branchings leads to a smaller $\vec{p}_T$ at each individual branching. The scalar E_T sum of recoiling partons may well be somewhat increased with more branchings included, but the vector p_T sum, i.e. the W p_T, is reduced because emissions with different azimuthal angles partly cancel. (Specifically, $\langle p_{TW}\rangle$ is maximal if only the hardest branching on each of the two incoming quark legs is included.) This conjecture is confirmed in Fig. 4, where PYTHIA results are compared without ordering, with Q^2 ordering, and with Q^2 + angular ordering; the latter alternative is based on a rather simplified scheme for including the additional coherence constraints in HERWIG.

The treatment of coherence effects is not the only difference between the programs (see [21] for some related discussion). Just about any program can still fit the data, since the absolute level of the predictions can be adjusted by the choice of Λ value or of maximum virtuality. Much of these uncertainties divide out if one takes the ratio of $\langle p_{TW}\rangle$ at two energies, 2 TeV and 630 GeV, say. (Even better would have been data at some lower energy, like 300 GeV, but probably this is unfeasible.) One then obtains 1.20 for WIZJET, 1.53 for PYTHIA, 1.64 for ISAJET and 1.70 for HERWIG. When data at 2 TeV become available, it should therefore be possible to discriminate between WIZJET and the other three. If the latter three are favoured, as seems likely, this might be taken as support for the concept of coherence although, to be fair, the separation between WIZJET and the others is much larger than can be explained by coherence differences alone. This point is illustrated by the energy dependence of the scalar E_T sum of recoiling partons, Fig. 5. The increase is seen to be slower in WIZJET than in the other programs, while the results in Fig. 4 would indicate that inclusion of Q^2 ordering or not should lead to the same results. The outlook is rather bleak for going one step further, and also establish the "new" angular ordering type of coherence in HERWIG, in addition to the Q^2 ordering one: no good physical signal has been found. (Despite a significant reduction in the number of branchings when angular ordering is imposed in PYTHIA, the final hadronic state looks just about the same.)

The actual shape of the p_{TW} spectrum is shown in Fig. 6 for 630 GeV. Note that the ISAJET spectrum is strongly peaked at the origin; the histogram binning does not resolve the structure of the innermost 1 GeV. It is easy to show that this is related to the Q_0 cutoff of the shower evolution, i.e. the virtuality below which partons are assumed not to branch any more. In ISAJET, Q_0 = 6 GeV, which leads to a significant probability that no branchings at all take place, and thus a p_{TW} that only comes from primordial k_T contributions. The other programs have $Q_0 \sim 1 - 2$ GeV, and show no corresponding behaviour, although they internally differ, with WIZJET having the largest tail out to large p_T, and the PYTHIA spectrum peaking at the lowest p_{TW}.

The p_T spectrum of associated jets is shown in Fig. 7, using a cluster algorithm with E_{Tmin} = 5 GeV and R = 1. Differences are visible, although the three programs studied here are all consistent with data (taking into account acceptance etc.). The larger Q_0 cutoff in ISAJET is mirrored in a more central production (in rapidity) of partons and jets, which carries over to the inclusive $dE_T/d\eta$ spectrum of hadrons, and also the charged rapidity distribution $dn_{ch}/d\eta$, Fig. 8. Note that this is despite large nonperturbative effects: the $\langle\Sigma E_T\rangle$ is increased by more than a factor 2 when moving from partons to hadrons.

Already current data probably contradict the p_{TW} spectrum of ISAJET, and the $dE_T/d\eta$ spectrum should be easy to test. If the experience with final state showers in e^+e^- annihilation is used as a guide [14], we expect both observables independently to point to the need for a lower cutoff Q_0. This might seem like a trivial enough retuning of ISAJET but, because the independent fragmentation ansatz is not stable with respect to collinear emission, probably rather significant modifications would become necessary.

3.2. QCD Jet Production

In this section we consider multijet production in the context of an underlying 2→2 parton scattering, i.e. the dominant high-p_T jet source. The basic two-jet picture is smeared by initial and final state radiation and by fragmentation, so that the p_T of the hard interaction is not truly a physical observable. For convenience, the Monte Carlo runs are still based on the selection of a minimum p_{Thard} as the only requirement. Some figures might therefore be somewhat different, depending on the experimental selection criteria, but this should hardly affect relative dissimilarities between

programs. Two standard scenarios are frequently referred to, 630 GeV $p\bar{p}$ collisions with p_{Thard} > 50 GeV, and 2 TeV $p\bar{p}$ ones with p_{Thard} > 100 GeV. In both cases jet finding is with E_{Tmin} = 10 GeV and R = 1, unless otherwise stated.

The charged multiplicity distribution is compared for four programs in Fig. 9. Average multiplicities, and fraction of multiplicity inside jets, are collected in Table 1. Note that multiplicities generally are lower in PYTHIA and HERWIG than in ISAJET and FRITIOF, and that the difference is increasing with energy. In ISAJET the number of charged particles with p_T > 1 GeV is still comparable with PYTHIA and HERWIG, i.e. the discepancy is mainly in the beam jet treatment. In the case of FRITIOF, there is a marked increase in multiplicity above p_T = 1 GeV, and a larger fraction of the total multiplicity is to be found inside jets, particularly at 2 TeV.

This incongruity between FRITIOF and the other three programs is not related to jet fragmentation as such, which is anyway the same string model as is used in PYTHIA, but to a significantly larger jet activity induced by initial and final state radiation, Fig. 10. As a simple (unphysical) measure, consider the ratio of the summed partonic E_T before fragmentation to twice the p_T of the basic hard 2→2 process. In the 2 TeV scenario, this ratio is on the average 1.35 in PYTHIA, 1.23 in HERWIG, 1.20 in ISAJET, but 1.66 in FRITIOF. Since part of the PYTHIA figure comes from the multiple interaction beam jet scenario, which is an extra component with no correspondence in the other programs, to first approximation the FRITIOF dipole radiation scheme contributes with three times as much additional E_T activity as the parton shower approach in the other three programs. If the FRITIOF scheme can be shown to be in disagreement with data, it probably does not reflect on the dipole scheme as such, but on the significant uncertainties in its application to the initial state part of the radiation. Without this high bremsstrahlung activity, FRITIOF would fail to account for the pedestal effect, however, since the beam jet structure itself is so clean.

Among the other three programs, generally HERWIG is the one with least jet activity and ISAJET the one with most. Differences are small compared with inherent uncertainties like Λ scale or maximum Q^2 value, however, and can therefore not in a simple way be ascribed to any underlying physics reasons. More information is then obtained by considering how the number of jets depend on R, the opening angle of the jet cone, Fig. 11. When R is decreased, a subjet structure can be resolved, so that more jets may be reconstructed.

Concurrently, the jet energy goes down, so that more potential jets fail the $E_{Tjet} > E_{Tmin} = 10$ GeV requirement. At 2 TeV, the former mechanism is the more important one for PYTHIA and HERWIG, for the R range considered, while the two balance each other for R < 0.5 in ISAJET. This difference is characteristic of the use of a higher Q_0 parton shower cutoff in ISAJET than in PYTHIA and HERWIG (as has been confirmed by running PYTHIA with the ISAJET cutoff value), cf. section 3.1, i.e. there is not as much subjet structure to be resolved at low R in ISAJET as in the other two. Experimental studies along these lines would be very interesting. The results with FRITIOF are again rather dissimilar, and at 2 TeV reflect the large number of jets around 10 GeV, which are lost as R is reduced.

The fact that the number of jets varies between programs does not necessarily mean that the internal structure of jets is all that unlike. The average p_T flow around the jet axis is very similar in the programs, Fig. 12, and so is the average p_T-p_T-weighted two-particle angular correlation inside jets, Fig. 13. In both of these cases, it would have been natural to expect differences related to the unlike Q_0 cutoffs in the programs, as in the W studies or in Fig. 11. Likely, inherent differences are smeared out by the averaging procedure over many events. Unfortunately, Figs. 12 and 13 are only two examples among many (not shown here) where it was difficult to draw any interesting conclusions.

In [30] a disparity was found between ISAJET and PYTHIA, where PYTHIA was shown to contain more events with little energy in a R = 1 cone around the "true" scattered parton direction. This likely comes from somewhat more hard parton shower branchings in PYTHIA, where the original parton is split into two (or more), which end up on opposite sides outside the R = 1 cone around their center of gravity. It is gratifying to note that this difference between the program still remains, 3 years later, Fig. 14. The newcomer HERWIG places itself squarely in between ISAJET and PYTHIA.

Unfortunately, a "true" parton direction is not a physical observable. Indeed, the exact definition of this direction is not necessarily the same in any two of the programs considered. Instead a more realistic algorithm is here proposed. Transverse sphericity S_T is defined by an ordinary sphericity search constrained to the transverse momentum plane, with normalization so that $0 < S_T < 1$:

$$S_T = 2 \min_{|\bar{n}|=1} \frac{\sum_i (\bar{p}_T \cdot \bar{n})^2}{\sum_i \bar{p}_{Ti}^2} \tag{1}$$

S_T distributions are shown in Fig. 15; the similarity indicates comparable amounts of hard three-jets in the programs. The details are slightly different, however, with PYTHIA having somewhat more large S_T and small S_T events and fewer in between.

The associated $\bar{n}$ axis divides the event in two transverse hemispheres. A hemisphere center is defined, in azimuth just in the middle of the allowed range, i.e. transverse to $\bar{n}$, in pseudorapidity by using the p_T^2-weighted average

$$\langle\eta\rangle = \frac{\sum_i \bar{p}_{Ti}^2 \eta_i}{\sum_i \bar{p}_{Ti}^2} \tag{2}$$

of all the particles in the given hemisphere. (Needless to say, both S_T and $\langle\eta\rangle$ could be replaced by quantities linear in p_T, for use with calorimeter information.) The p_T flow around the hemisphere center only shows minor differences between the programs, Fig. 16. For each given opening angle R around the hemisphere center, it is possible to study the distribution of the fraction of ΣE_T inside the cone to the total ΣE_T in the hemisphere. The result is shown in Fig. 17 for R = 1.

In this language, the original observation in [30] is that the PYTHIA distribution has a larger tail down to low values than the ISAJET one. While still true, the discrepancy is certainly less impressive in Fig. 17 than originally, i.e. the introduction of an experimentally reproducible procedure has reduced the signal. The distribution as such still contains major differences between programs, and would therefore be interesting to study further. In particular, if the bulk of the distributions are considered, rather than the tails, it is seen that FRITIOF and ISAJET events contain a larger fraction of the hemisphere energy outside the R = 1 cone than does HERWIG or PYTHIA events. An open question is to what extent these results would be affected by a different α_s choice or a different maximum virtuality in the shower evolution, i.e. by effects reflecting an uncertainty in the size of higher order QCD corrections rather than in the underlying physics scenarios as such.

3.3. Quark versus Gluon Jets

There are two reasons why gluon jets are expected to be softer than quark ones, both related to the double colour charge of the gluon. First, on the perturbative level, $g \to gg$ branchings are enhanced compared to $q \to qg$ ones. Second, in string and cluster fragmentation models, two chains of hadrons are stretched by a gluon, but only one by a quark. In independent fragmentation models, like ISAJET, COJETS, EUROJET and FIELDAJET, gluon and quark fragmentation are in principle separately tunable, but normally a gluon is just fragmented like a quark with flavour chosen at random, so that the second reason is not there.

Experimentally, UA1 has already found gluon jet fragmentation to be softer than the quark one [12], by the amount predicted in PYTHIA [31]. As Fig. 18 shows, HERWIG gives similar results, whereas ISAJET has a far smaller q/g dissimilarity, which probably could not be reconciled with data. The angular energy flow also contains q/g differences, Fig. 19. This means that the energy of a gluon jet is systematically underestimated compared to that of a quark jet, so that the gluon jet fragmentation may seem to be harder than it really is. Even with rather restrictive jet energy definitions, like only using charged particles with $p_T > 1$ GeV, the g/q difference still survives, Fig. 18b.

3.4. Particle Composition

Most programs contain fairly many tunable parameters for the particle composition simulation, and for programs like ISAJET these are tuned directly to fit hadron physics data. Therefore the predictive power is rather limited. In the Lund programs, parameters are tuned to e^+e^- data and nothing else. Then a number of discrepancies exist between PYTHIA predictions and ISR data. The K/π ratio for a single particle trigger above $p_T = 3$ GeV is 0.46, where models give at most 0.40 [32]. The p/π ratio is even more problematic: at large p_T values, PYTHIA overestimates p production, but fails to account for the large proton signal at intermediate p_T, $p_T \approx 1 - 3$ GeV, which has been interpreted as evidence for diquark scattering [33].

The only other program (excepting FRITIOF, which should be similar to PYTHIA) for which nontrivial statements could be made is HERWIG. Again the high-p_T behaviour is constrained by e^+e^- data. Interestingly, HERWIG contains a

mechanism for explaining the "diquark scattering" signal: since cluster decay is assumed to be completely isotropic in the rest frame of a cluster, the cluster that contains a beam remnant diquark can produce a reasonably high-p_T proton in its decay. The p/charged$^+$ ratio in Fig. 20 illustrates this point, although obviously any definite conclusions should be based on a detailed simulation of experimental trigger conditions. It could be that, even if the inclusive p rate is about right as a function of p_T, these protons are produced in the wrong angular region of the events.

3.5. String Effects

In string and cluster fragmentation models, strings or chains of clusters are stretched between the final state partons, with each quark (or diquark) attached to one such string/chain and each gluon to two, cf. section 2.4. Depending on whether a string is stretched between two jets or not, the angular range between the jets will contain more or less many particles, on the average. In e^+e^- annihilation, this kind of effects is well established [34], and has been used as very strong evidence against the independent fragmentation framework. The situation is considerably more messy in hadron physics.

Strings and string effects appear already as a consequence of the colour flow in the hard $2 \to 2$ scattering, as exemplified in Fig. 2. Further effects appear with the additional partons produced by initial and final state radiation. The dynamics of hard scatterings and parton branchings favour configurations where two partons nearby in momentum space also share a colour-anticolour pair, and thus are connected by a string (or cluster chain). Particle production thereby comes to be asymmetrically distributed around the true parton direction, with more particles on the side towards the nearest neighbouring parton. Were the true parton direction known, string effects could have been readily visible also in hadron physics. Unfortunately, the experimentally reconstructed jet axes are also affected by the asymmetrical particle distribution, so that two nearby partons are systematically reconstructed as being even closer to each other than they really are.

In events with three high-p_T partons, the visible three-jettiness of the final hadronic event is thus smaller with string or cluster fragmentation than with independent fragmentation. In model comparisons, this can be compensated by using larger α_s values in the former case and smaller in the latter. For the

experimental α_s determinations based on the ratio of events with three and two high-p_T jets, the separation between the string and independent fragmentation α_s values is typically 60% at ISR energies and 15% at Sp$\bar{p}$S ones [35]. It is therefore important to remember that the difficulty of observing string effects does not imply that the effects on experimentally extracted quantities need be small. Also, it seems likely that a dedicated study, where high-p_T events are projected onto the transverse momentum plane and then analyzed along the general lines used for e^+e^- events, could directly establish the presence of string effects.

Here, an alternative study is instead proposed, which has no counterpart in e^+e^- annihilation, since it is directed towards the study of the strings stretched between the two hard scattered partons and the beam remnants, i.e. strings that would not be visible in a projection onto the transverse momentum plane. For simplicity, only qg→qg scatterings were studied, but this is not an essential assumption. The algorithm is as follows. Find the two hard jets by a cluster algorithm, with R = 1. Then only consider particles inside the jets which have $0.5 < p_T < 1$ GeV, and plot their distribution in azimuth χ around the jet axis, with $\chi = 0$ corresponding to direction "outwards" towards the beam jets. For "round" jets the distribution in χ should then be flat. In fact, simple phase space arguments give more particle production from the "underlying event" at smaller rapidities, and thus favour $\chi > 90^\circ$. Thus, in ISAJET $\langle\chi-90^\circ\rangle = 4.0^\circ$. String effects work in the opposite direction, since a string stretched out towards the nearest beam remnant is more boosted than a string to the beam remnant in the other hemisphere or to the other central parton. In PYTHIA $\langle\chi-90^\circ\rangle = 1.1^\circ$ and in HERWIG 0.2°. The values above are averages over the quark and the gluon jet, but the same pattern is actually visible in the two separately. Studies of this kind should therefore be pursued.

Fortunately, a more direct proof of string effects in hadron collisions already exists, coming from charm production. With the c quark Feynman x spectrum given by perturbative QCD, the independent fragmentation approach involves folding the quark spectrum with a c→D fragmentation function, such that the final D spectrum is more strongly peaked at $x_F = 0$ than the c one. In string (or cluster) fragmentation, on the other hand, a charm quark is connected to a beam remnant with a string, and the D meson produced out of this field may be dragged along to a larger x_F than the original c quark [36]. Indeed, detailed calculations give quite good agreement with data for different charmed particles [37], although with a few half failures that

remain to be understood.

3.6. Low-p_T Aspects

The thrust of this study has been towards high-p_T physics. Indeed, several of the programs discussed are not intended for the study of minimum bias events; what is offered is parametrizations rather than models. The only two programs which claim to include low-p_T and high-p_T physics in one single unified model are PYTHIA and FRITIOF.

In PYTHIA, the concept of multiple interactions plays a central rôle for this unified description [27]. The philosophy is that, since hadrons are composite objects, the possibility exists of several (disjoint) parton-parton interactions when the two hadrons collide. Further, central collisions leads to a larger average number of interactions than peripheral ones. Fluctuations in the number of interactions per event is one of the main sources for obtaining a multiplicity distribution much broader than the naive Poissonian one. In order to agree with the data, it is necessary to assume parton-parton interactions down to a transverse momentum cutoff scale of roughly 2 GeV. (In practice, there is no sharp cutoff of perturbative QCD, but rather a smooth turnoff.) The main consequence of this low value is that the possibility of two separately visible semihard interactions is not negligible. None of the other programs allows for the presence of multiple interactions. In some programs it could be added by brute force, but it is nothing required by internal consistency, as is the case for PYTHIA. So far, the verdict is not at hand. AFS has published evidence for multiple interactions [38], in good agreement with PYTHIA predictions (which are significantly above naive expectations, due to the impact parameter effects), but preliminary UA2 studies do not show any signal [39].

Another interesting observable is the pedestal effect, and how the height of the pedestal depends on the E_T of the jet. This height is defined as the $dE_T/d\eta$ flow in the region $1 \leq |\eta - \eta_{jet}| \leq 2$ and $|\phi - \phi_{jet}| \leq 90^\circ$. In the UA1 data, the pedestal height increases from minimum bias events up to $E_{T\,jet} \approx 10$ GeV, and thereafter stays more or less constant [40]. In PYTHIA, the behaviour up to 10 GeV is partly due to an increase in initial and final state radiation, but mainly to a shift towards events with smaller impact parameter and hence more interactions. Above 10 GeV, events are already maximally biased in impact parameter, and a small drop in underlying event activity is related

to the transition from $gg \to gg$ to $q\bar{q} \to q\bar{q}$ interactions.

The HERWIG authors, on the contrary, find no need for multiple interactions, but rather conclude that perturbatively calculable QCD bremsstrahlung, in combination with a suitable soft underlying event structure, is enough to explain the data [41]. An interesting test is suggested to check the validity of the HERWIG scenario. The pedestal is, event-by-event, subdivided into a left region $\eta_{jet}-2 < \eta < \eta_{jet}-1$ and a right one $\eta_{jet}+1 < \eta < \eta_{jet}+2$. The transverse energies in these two regions are denoted ω_T^L and ω_T^R, so that the ordinary pedestal height ω_T^{ped} is the average of the two. To leading order in α_s, where only $2 \to 3$ matrix elements contribute, only one of ω_T^L and ω_T^R is nonvanishing. For a uniform minimum bias background, on the other hand, ω_T^L and ω_T^R should be comparable. It is therefore suggested that a study of the energy dependence of

$$\omega_T^{dif} = \frac{1}{2} |\omega_T^L - \omega_T^R| \tag{3}$$

and

$$\omega_T^{min} = \min(\omega_T^L, \omega_T^R) = \omega_T^{ped} - \omega_T^{dif} \tag{4}$$

would help separate the perturbative and the "true minimum bias" contributions. We agree that such a study should be made, but urge caution as to what conclusions should be drawn from it. In particular, if multiple interactions indeed exist in nature, a jet from one of these extra interactions would, in the procedure above, be indistinguishable from a bremsstrahlung jet. The interpretation of the amount of true bremsstrahlung needed for a given ω_T^{dif} would therefore be model-dependent.

As in high-p_T physics in general, it is probable that the verdict on the underlying event models will be based, not on any one single observation, but rather on the demand of consistently explaining a host of different observables: multiplicity distributions, forward-backward correlations, rapidity and p_T distributions and correlations, minijet and multi-minijet phenomenology, pedestals, etc.

4. Summary

In this paper, I have reviewed Monte Carlo programs for the simulation of high-p_T events. Ideally, these programs ought to have been nothing but computer implementations of known properties of the standard elctroweak and

strong theories. Unfortunately, such knowledge is very limited. In reality the programs therefore are, at best, works of art and, at worst, collections of cookbook recipes. (Or the other way around, depending on taste.) This also means that there is no simple answer to the question which is the "best" program. Only comparisons with data can help tell.

To date, essentially no attempts have been made to confront different high-p_T programs with the same data. This compares quite unfavourably with e^+e^- annihilation physics. In particular, one may fear that the virtual monopoly of ISAJET is symptomatic of a lack of curiosity. In the defence of our experimental colleagues, it should be said that the task is considerably more difficult than in e^+e^- annihilation. The number of tunable parameters is so large that essentially every program can be made to agree with any one specific piece of data. When many different observations are put together, it should still be possible to tell quite a lot about the Monte Carlos on the market.

A number of studies have been suggested here. The $\langle p_{TW} \rangle$ evolution between 630 GeV and 2 TeV is different in the WIZJET initial state radiation routine from that in others. The large cutoff used both for initial and final state radiation in ISAJET can be tested, in the former case by looking at the p_{TW} spectrum, or the particle rapidity distribution in W events, in the latter by considering the number of jets in an event as a function of the jet opening cone. The jet structure in FRITIOF events is sufficiently distinct that several tests can be used. Dissimilarities between quark and gluon jet have already been noted in the data, and probably already discriminates against gluon jet models in some programs. The observation of string effects is nontrivial, but not entirely impossible. A major disappointment is maybe that PYTHIA and HERWIG are so similar, despite the extra initial state radiation coherence constraints in HERWIG. The rather special flow of baryon numbers in HERWIG would be of interest to study, however. The structure of the underlying event is also quite different. In particular, PYTHIA is the only program to include multiple semihard interactions. A study on this subject remains one of the major challenges of Collider physics.

With a fruitful interplay between experimentalists and Monte Carlo builders, the future therefore looks rather promising for deepening our understanding of high-p_T processes.

References

1. F.E. Paige, S.D. Protopopescu, in Physics of the Superconducting Super Collider 1986, eds. R. Donaldson, J. Marx (1987), p. 320
2. H.-U. Bengtsson, T. Sjöstrand, Computer Phys. Comm. 46 (1987) 43
3. G. Marchesini, B.R. Webber, Cavendish-HEP-87/8 and UPRF-87-212, Cavendish-HEP-87/9 (1987)
4. R. Odorico, Nucl. Phys. B228 (1983) 381, Computer Phys. Comm. 32 (1984) 139
5. B. Andersson, G. Gustafson, B. Nilsson-Almqvist, Nucl. Phys. B281 (1987) 289, LU TP 87-6 (1987)
   B. Nilsson-Almqvist, E. Stenlund, Computer Phys. Comm. 43 (1987) 387
6. A. Ali, B. van Eijk, I. ten Have, Nucl. Phys. B292 (1987) 1 and references therein
7. R.D. Field, G.C. Fox, R.L. Kelly, Phys. Lett. 119B (1982) 439
   R.D. Field, Nucl. Phys. B264 (1986) 687
8. J. Ranft, SSC-Report 150 (1987)
   J. Ranft, P. Aurenche, F. Bopp, A. Capella, K. Hahn, J. Kwiecinski, P. Maire, J. Tran Thanh Van, SSC-149 (1987)
9. L.V. Gribov, E.M. Levin, M.G. Ryskin, Phys. Rep. 100 (1983) 1
10. A.H. Mueller, Phys. Lett. 104B (1981) 161
    B.I. Ermolaev, V.S. Fadin, JETP Lett. 33 (1981) 269
11. M. Ciafaloni, Nucl. Phys. B296 (1987) 249
12. UA1 Collaboration, G. Arnison et al., Nucl. Phys. B276 (1986) 253
13. T. Sjöstrand, Computer Phys. Comm. 39 (1986) 347
    T. Sjöstrand, M. Bengtsson, Computer Phys. Comm. 43 (1987) 367
14. T. Sjöstrand, International Journal of Modern Physics A3 (1988) 751 and references therein
15. T.D. Gottschalk, in From Colliders to Super Colliders, eds. V. Barger, F. Halzen (World Scientific, Singapore, 1987), p. 503
16. P. Nason, S. Dawson, R.K. Ellis, Nucl. Phys. B303 (1988) 607
17. E. Eichten, I. Hinchliffe, K. Lane, C. Quigg, Rev. Mod. Phys. 56 (1984) 579, 58 (1986) 1065
18. D. Duke, J.F. Owens, Phys. Rev. D30 (1984) 49
    J.F. Owens, Phys. Rev. D30 (1984) 943
19. A.D. Martin, R.G. Roberts, W.J. Stirling, Phys. Rev. D37 (1988) 1161
    M. Diemoz, F. Ferroni, E. Longo, G. Martinelli, Z. Physik C39 (1988) 21

20. W.-K. Tung, in Physics Simulations at High Energy, eds. V. Barger, T. Gottschalk, F. Halzen (World Scientific, Singapore, 1987), p. 601
21. T. Sjöstrand, Phys. Lett. 157B (1985) 321
    M. Bengtsson, T. Sjöstrand, M. van Zijl, Z. Physik C32 (1986) 67
22. R.D. Field, T.D. Gottschalk, Phys. Rev. D35 (1987) 875
23. Ya.I. Azimov, Yu.L. Dokshitzer, V.A. Khoze, S.I. Troyan, Phys. Lett. 165B (1985) 147, Leningrad preprint 1051 (1985)
    G. Gustafson, Phys. Lett. 175B (1985) 453
    G. Gustafson, U. Pettersson, LU TP 87-9 (1987)
24. UA5 Collaboration, G.J. Alner et al., Nucl. Phys. B291 (1987) 445
25. V.A. Abramovski, O.V. Kancheli, V.N. Gribov, in Proc. of XVI International Conference on High Energy Physics, eds. J.D. Jackson, A. Roberts, R. Donaldson, Vol. 1, p. 389
26. A. Capella, J. Tran Thanh Van, Phys. Lett. 114B (1982) 450, Z. Physik C18 (1983) 85, C23 (1984) 165
27. T. Sjöstrand, M. van Zijl, Phys. Rev. D36 (1987) 2019
28. see e.g.
    Physics of the Superconducting Super Collider 1986, eds. R. Donaldson, J. Marx (1987)
    From Colliders to Super Colliders, eds. V. Barger, F. Halzen (World Scientific, Singapore, 1987)
    Experiments, Detectors, and Experimental Areas for the Supercollider, ed. R. Donaldson, M.G.D. Gilchriese (World Scientific, Singapore, 1988)
29. UA1 Collaboration, G. Arnison et al., Lett. Nuovo Cimento 44 (1985) 1
    UA2 Collaboration, J.A. Appel et al., Z. Physik C30 (1986) 1
30. B. Cox et al., in Supercollider Physics, ed. D.E. Soper (World Scientific, Singapore, 1986), p. 120
31. T. Sjöstrand, in Proceedings of the 1984 Snowmass SSC Summer Study, eds. R. Donaldson, J. G. Morfín, p. 84
32. W.M. Geist, Phys. Lett. 196B (1987) 251 and references therein
33. A. Breakstone et al., Phys. Lett. 147B (1984) 237, Z. Physik C28 (1985) 335
    S. Ekelin, S. Fredriksson, Phys. Lett. 149B (1984) 509
34. JADE Collaboration, W. Bartel et al., Phys. Lett. 101B (1981) 129, Z. Physik C21 (1983) 37, Phys. Lett. 134B (1984) 275
    TPC/2γ Collaboration, H. Aihara et al., Z. Physik C28 (1985) 31
    TASSO Collaboration, M. Althoff et al., Z. Physik C29 (1985) 29
35. M. Bengtsson, T. Sjöstrand, M. van Zijl, Phys. Lett. 179B (1986) 164
36. B. Andersson, H.-U. Bengtsson, G. Gustafson, LU TP 83-4 (1983)
37. NA27 LEBC-EHS Collaboration, M. Aguilar-Benitez et al., Phys. Lett. 161B

(1985) 400, 164B (1985) 404

38. AFS Collaboration, T. Åkesson et al., Z. Physik C34 (1987) 163

39. M. Wunsch, talk at the XXIIIrd Rencontres de Moriond (1988)

40. UA1 Collaboration, C. Albajar et al., CERN-EP/88-29 (1988)

41. G. Marchesini, B. R. Webber, NSF-ITP-88-67 (1988)

Table 1

Charged multiplicity, fraction of this multiplicity found inside jets, and charged multiplicity with transverse momentum above 1 GeV, in 630 GeV and 2 TeV $p\bar{p}$ interactions, with p_{Thard} > 50 GeV and 100 GeV, respectively.

	PYTHIA	HERWIG	ISAJET	FRITIOF
630 GeV				
$\langle n_{ch} \rangle$	76	81	91	91
$\langle n_{ch} \rangle_{in\ jets} / \langle n_{ch} \rangle$	48%	42%	47%	50%
$\langle n_{ch}(p_T > 1\ GeV) \rangle$	19.5	21.3	19.7	24.0
2 TeV				
$\langle n_{ch} \rangle$	126	118	153	151
$\langle n_{ch} \rangle_{in\ jets} / \langle n_{ch} \rangle$	52%	50%	54%	69%
$\langle n_{ch}(p_T > 1\ GeV) \rangle$	34.5	35.2	35.0	50.7

Figure Captions

Fig. 1. Notation used in discussion of initial state parton showers.

Fig. 2. a) In PYTHIA and HERWIG, two different flows of colours are possible in a $qg \to qg$ scattering; the flow of each colour is denoted by a dashed line (note that, for simplicity, not all Feynman diagrams contributing to $qg \to qg$ scattering are shown).
b) These give rise to two different topologies for how strings (dashed) connect the scattered partons (3,4) and the beam remnants ($\bar{1},\bar{2}$).

Fig. 3. The average W transverse momentum as a function of CM energy.

Fig. 4. The average W transverse momentum and recoiling partonic transverse energy as a function of CM energy, for PYTHIA without coherence, with Q^2 ordering and with Q^2 plus angular ordering.

Fig. 5. The average recoiling partonic transverse energy in W events as a function of CM energy.

Fig. 6. The shape of the W transverse momentum spectrum at 630 GeV. For ISAJET, the sharp peak at small p_{TW} is shown averaged over the first histogram bin.

Fig. 7. The transverse momentum spectrum of jets in events containing a W (excluding W decay products).

Fig. 8. Inclusive pseudorapidity distributions in events containing a W (excluding the W decay products).
a) Partonic transverse energy flow.
b) Hadronic transverse energy flow.
c) Charged multiplicity flow.

Fig. 9. Charged multiplicity distributions in 2 TeV $p\bar{p}$ events with p_{Thard} > 100 GeV.
a) For all charged particles.

b) For charged particles with transverse momentum p_T > 1 GeV.

Fig. 10. Jet E_T spectrum, for jets with E_T > 10 GeV in a R = 1 opening cone, in 2 TeV $p\bar{p}$ events with p_{Thard} > 100 GeV.

Fig. 11. Number of jets with E_T > 10 GeV as a function of the jet opening cone R. The lower four curves refer to 630 GeV $p\bar{p}$ events with p_{Thard} > 50 GeV, the upper four to 2 TeV $p\bar{p}$ events with p_{Thard} > 100 GeV.

Fig. 12. Normalized p_T flow around jet axis, as a function of $\omega = ((\eta-\eta_{jet})^2 + (\phi-\phi_{jet})^2)^{1/2}$, for jets with E_T > 20 GeV in 630 GeV $p\bar{p}$ events with p_{Thard} > 50 GeV.

Fig. 13. Normalized transverse momentum correlations inside jets defined as for Fig. 12, with two-particle distance $\omega_{ij}^2 = (\eta_i-\eta_i)^2 + (\phi_i-\phi_i)^2$.

Fig. 14. Partonic transverse energy in a R = 1 cone around the "true" hard scattered parton direction, normalized to the naive p_T of this parton. 2 TeV $p\bar{p}$ events with p_{Thard} > 100 GeV.

Fig. 15. Transverse sphericity (S_T, eq. (1)) distributions in 2 TeV $p\bar{p}$ events with p_{Thard} > 100 GeV.

Fig. 16. Transverse momentum flow around hemisphere center, normalized to the total transverse energy in the hemisphere. This center is defined by the transverse sphericity axis and the p_T^2-weighted hadronic average pseudorapidity, eqs. (1) and (2). 2 TeV $p\bar{p}$ events with p_{Thard} > 100 GeV.

fig. 17. Fraction of total transverse energy of one hemisphere found within a R = 1 cone around the hemisphere center. Comments as for Fig. 16.

Fig. 18. Ratio of gluon to quark fragmentation functions in 630 GeV $p\bar{p}$ $qg \to qg$ events with p_{Thard} > 50 GeV.
a) For all particles inside a R = 1 jet cone.
b) For charged particles with p_T > 1 GeV inside a R = 1 jet cone; with jet energy defined by these particles only.

Fig. 19. Ratio of gluon to quark transverse energy flow at distance ω away from jet axis, in events as for Fig. 18.

Fig. 20. Proton fraction of positive particles as a function of transverse momentum for 63 GeV pp events with $p_{Thard} > 8$ GeV, in HERWIG and PYTHIA.

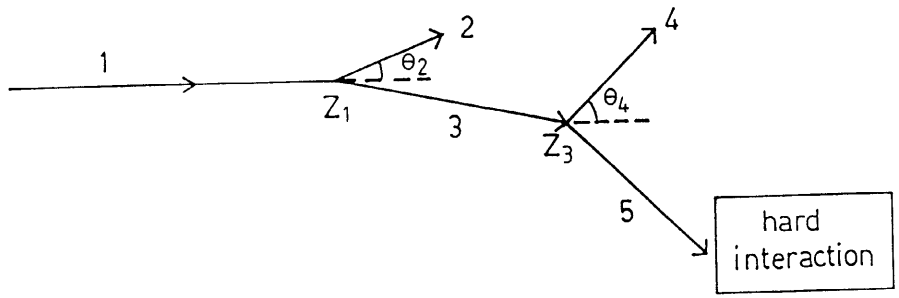

Fig. 1

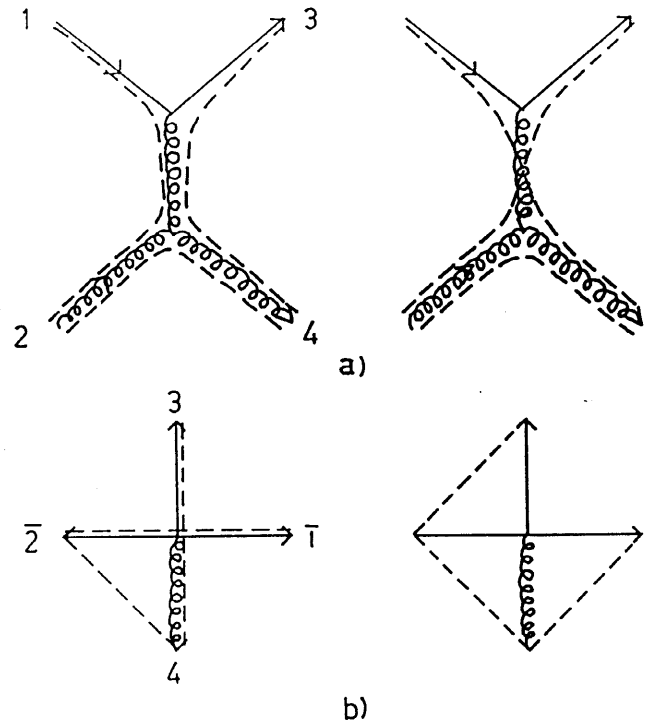

Fig. 2

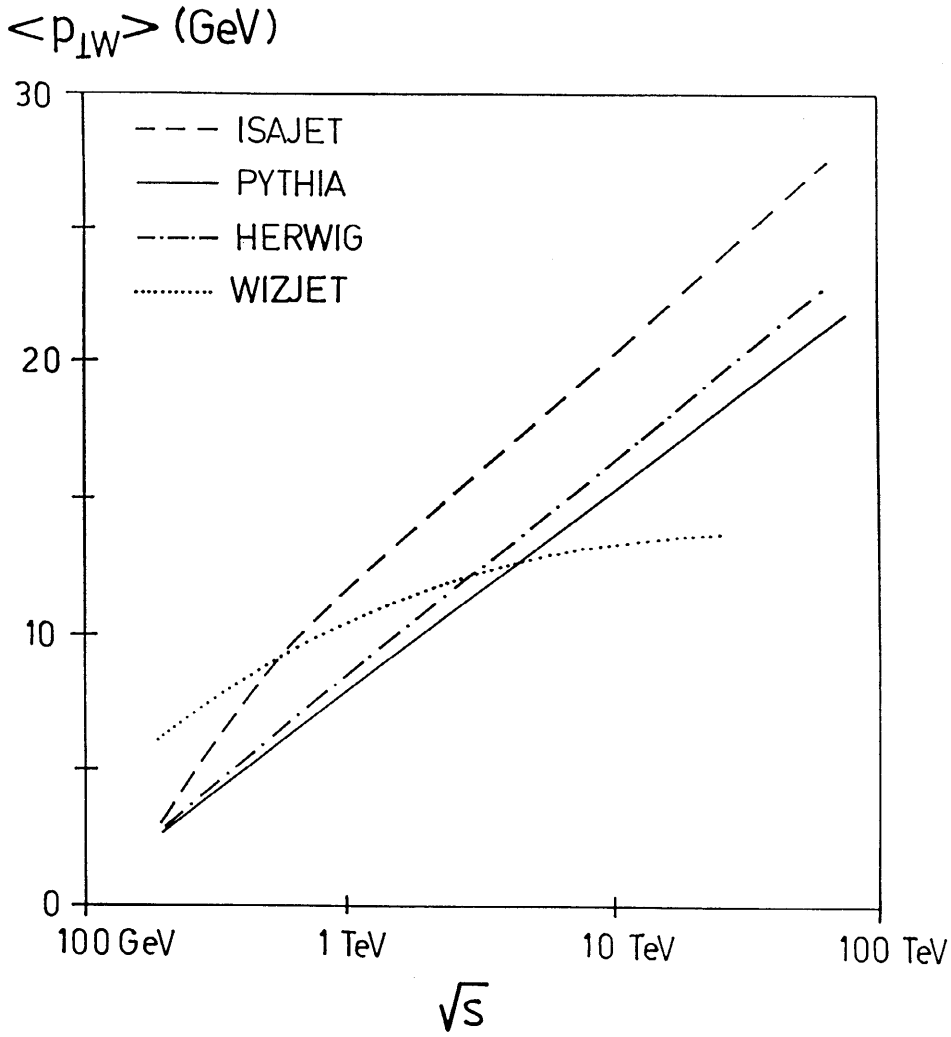
$<p_{\perp W}>$ (GeV)
30
20
10
0
ISAJET
PYTHIA
HERWIG
WIZJET
100 GeV
1 TeV
10 TeV
100 TeV
$\sqrt{s}$

Fig. 3

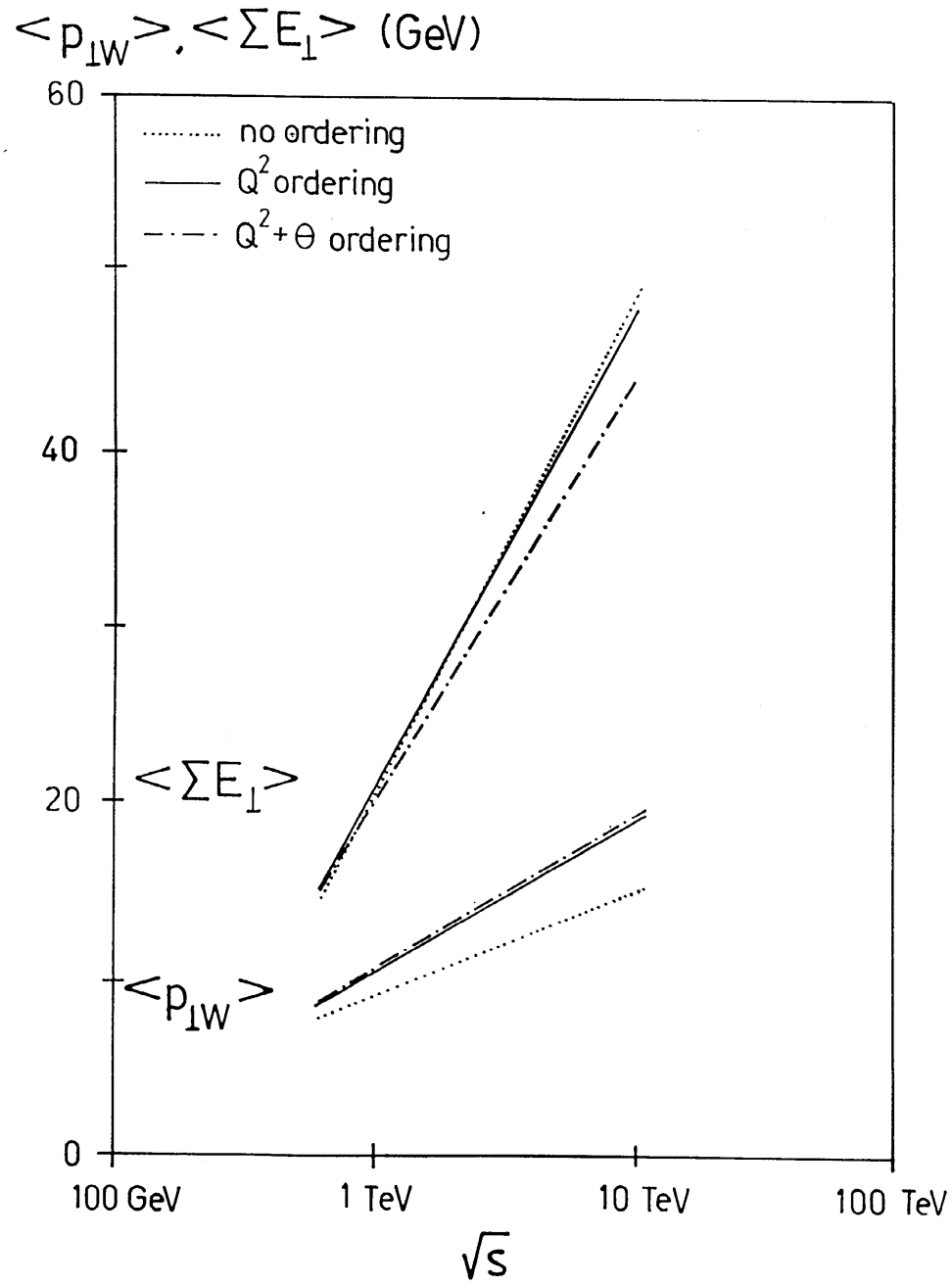
$<p_{\perp W}>, <\Sigma E_\perp>$ (GeV)
60
40
20
0
no ordering
Q^2 ordering
$Q^2+\Theta$ ordering
$<\Sigma E_\perp>$
$<p_{\perp W}>$
100 GeV
1 TeV
10 TeV
100 TeV
$\sqrt{s}$

Fig. 4

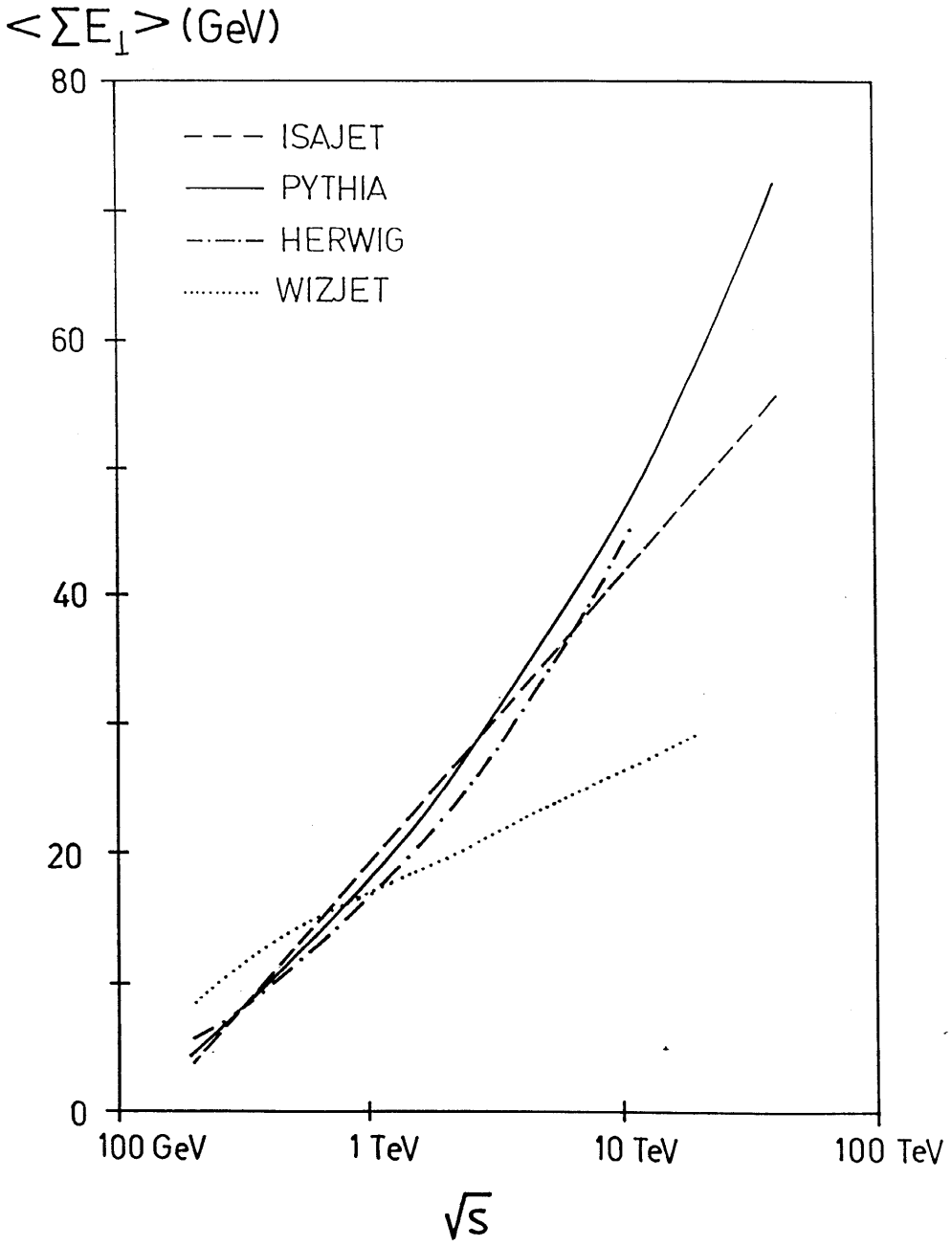
$<\sum E_\perp>$ (GeV)
80
60
40
20
0
ISAJET
PYTHIA
HERWIG
WIZJET
100 GeV
1 TeV
10 TeV
100 TeV
$\sqrt{s}$

Fig. 5

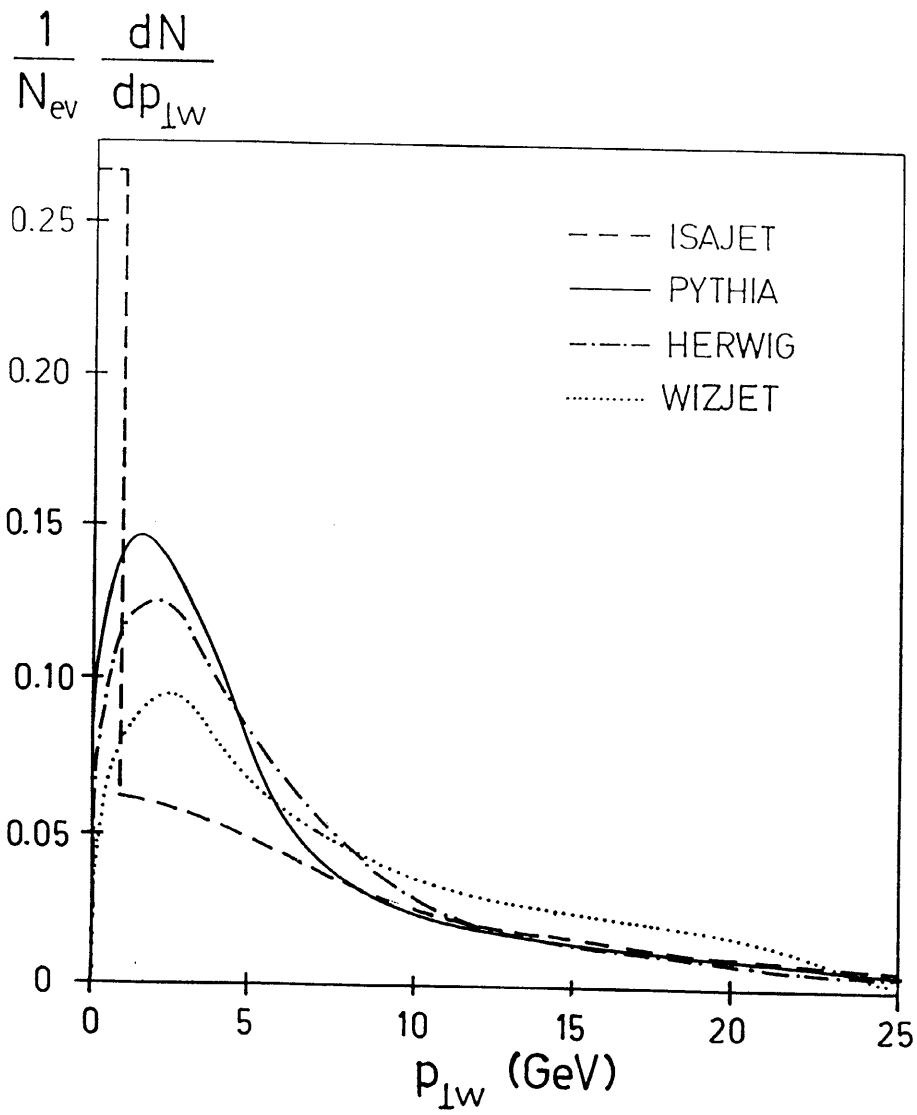
$\frac{1}{N_{ev}} \frac{dN}{dp_{\perp w}}$
0.25
0.20
0.15
0.10
0.05
0
ISAJET
PYTHIA
HERWIG
WIZJET
0
5
10
15
20
25
$p_{\perp w}$ (GeV)

Fig. 6

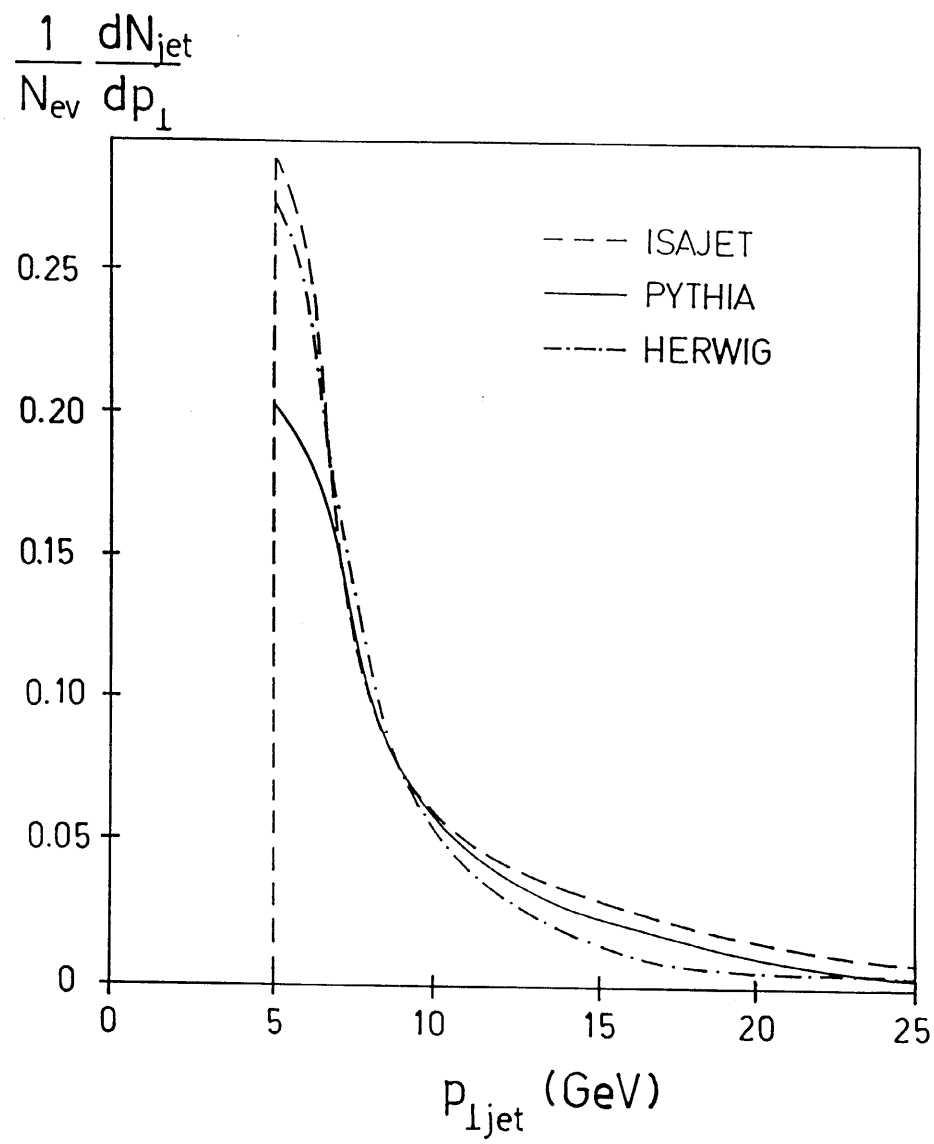
$\frac{1}{N_{ev}} \frac{dN_{jet}}{dp_\perp}$
0.25
0.20
0.15
0.10
0.05
0
0
5
10
15
20
25
$p_{\perp jet}$ (GeV)
ISAJET
PYTHIA
HERWIG

Fig. 7

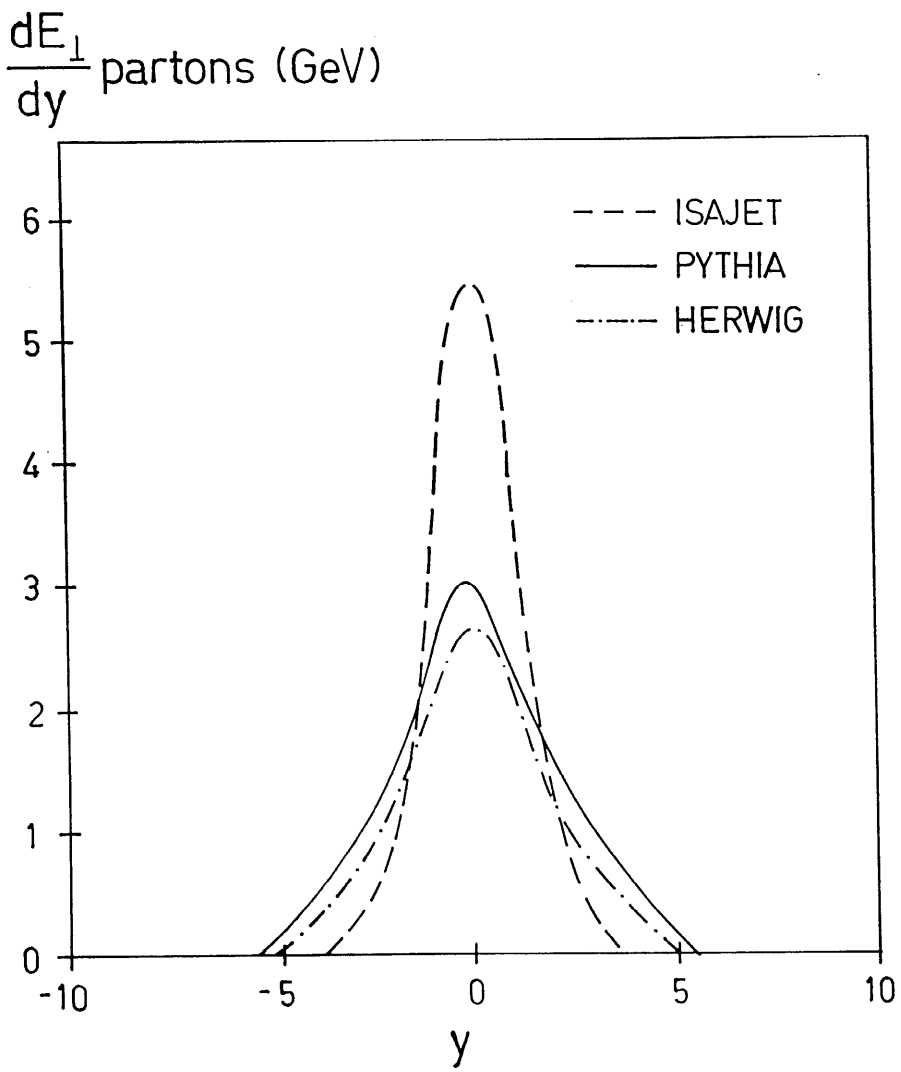
$\frac{dE_\perp}{dy}$ partons (GeV)
6
5
4
3
2
1
0
-10
-5
0
5
10
y
ISAJET
PYTHIA
HERWIG

Fig. 8a

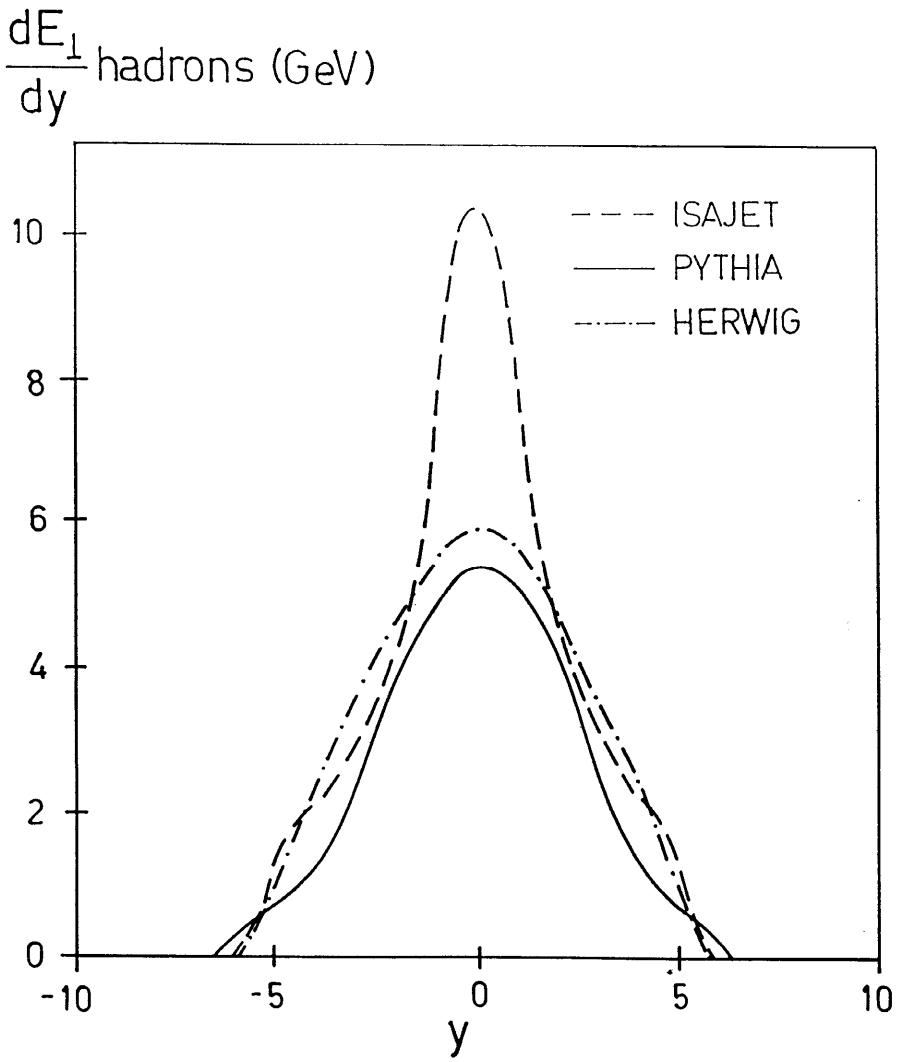
$\frac{dE_\perp}{dy}$ hadrons (GeV)
ISAJET
PYTHIA
HERWIG
10
8
6
4
2
0
-10
-5
0
5
10
y

Fig. 8b

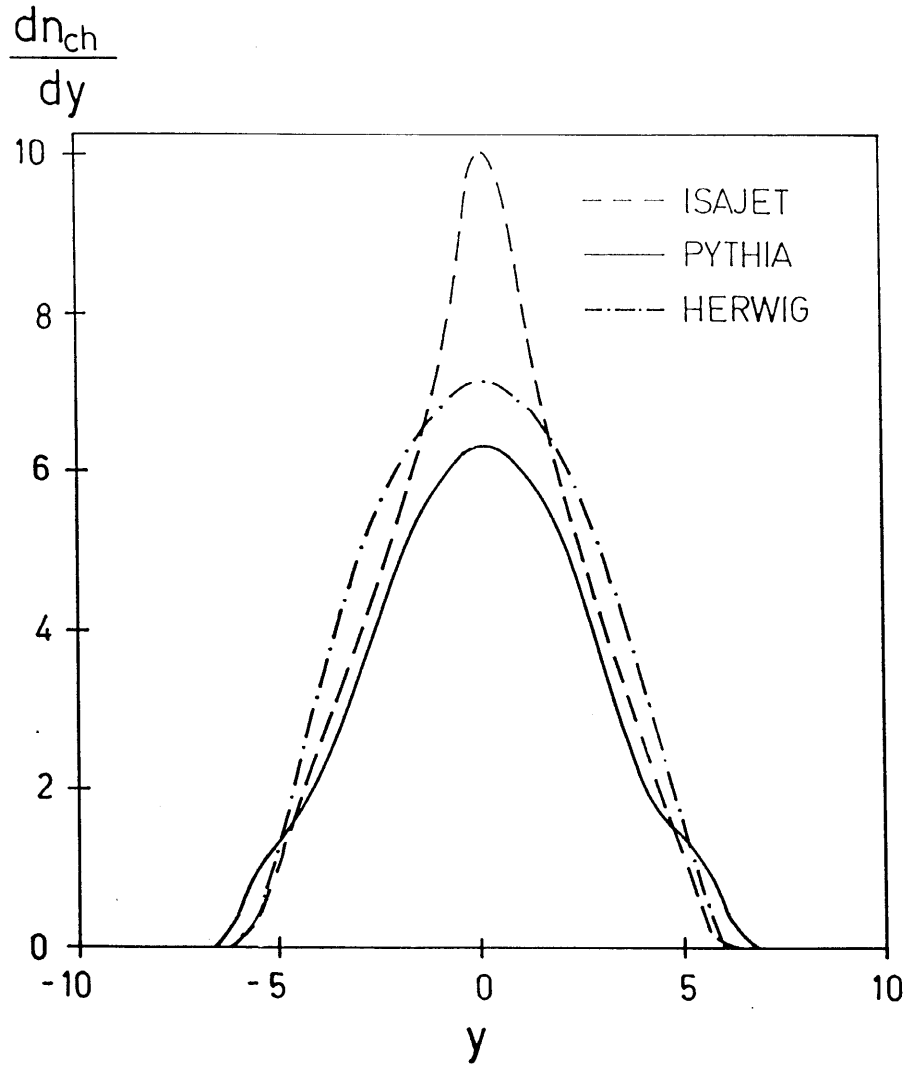
$\frac{dn_{ch}}{dy}$
ISAJET
PYTHIA
HERWIG
10
8
6
4
2
0
-10
-5
0
5
10
y

Fig. 8c

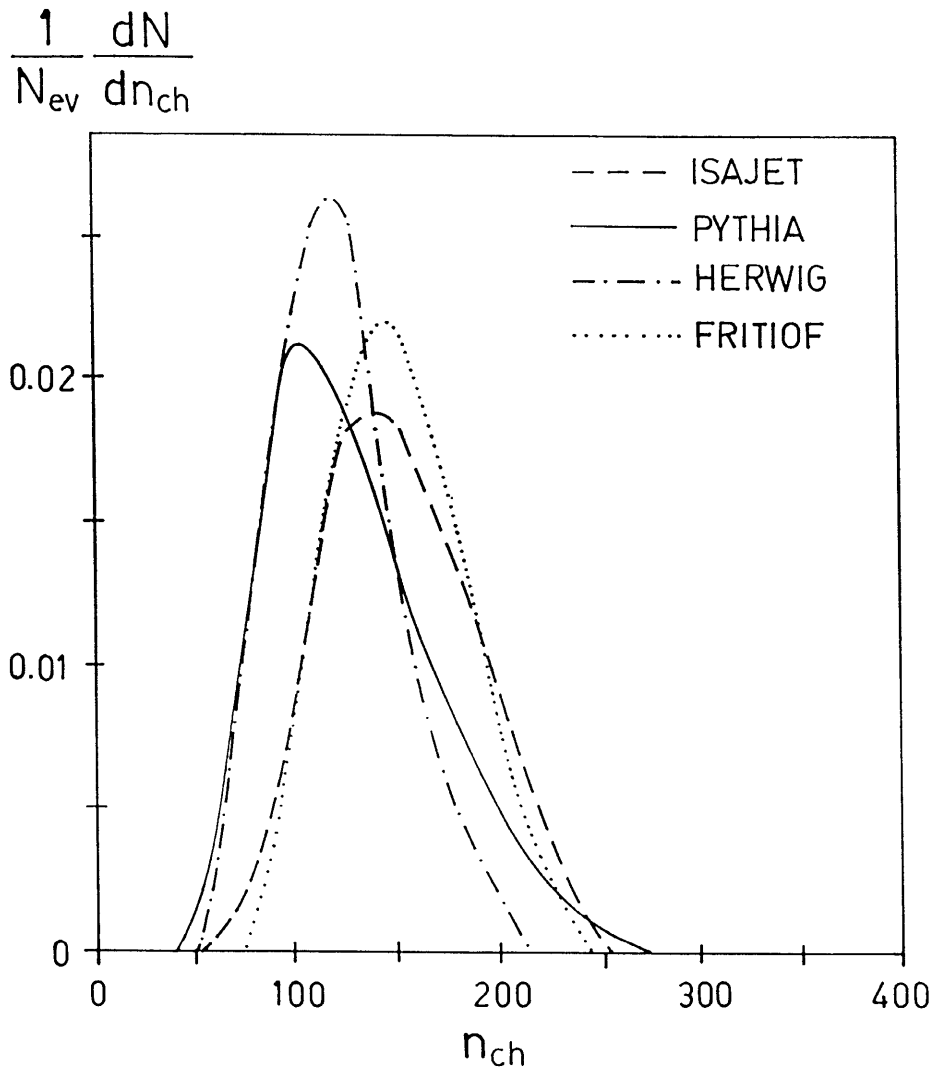
$\frac{1}{N_{ev}} \frac{dN}{dn_{ch}}$
ISAJET
PYTHIA
HERWIG
FRITIOF
0.02
0.01
0
0
100
200
300
400
n_{ch}

Fig. 9a

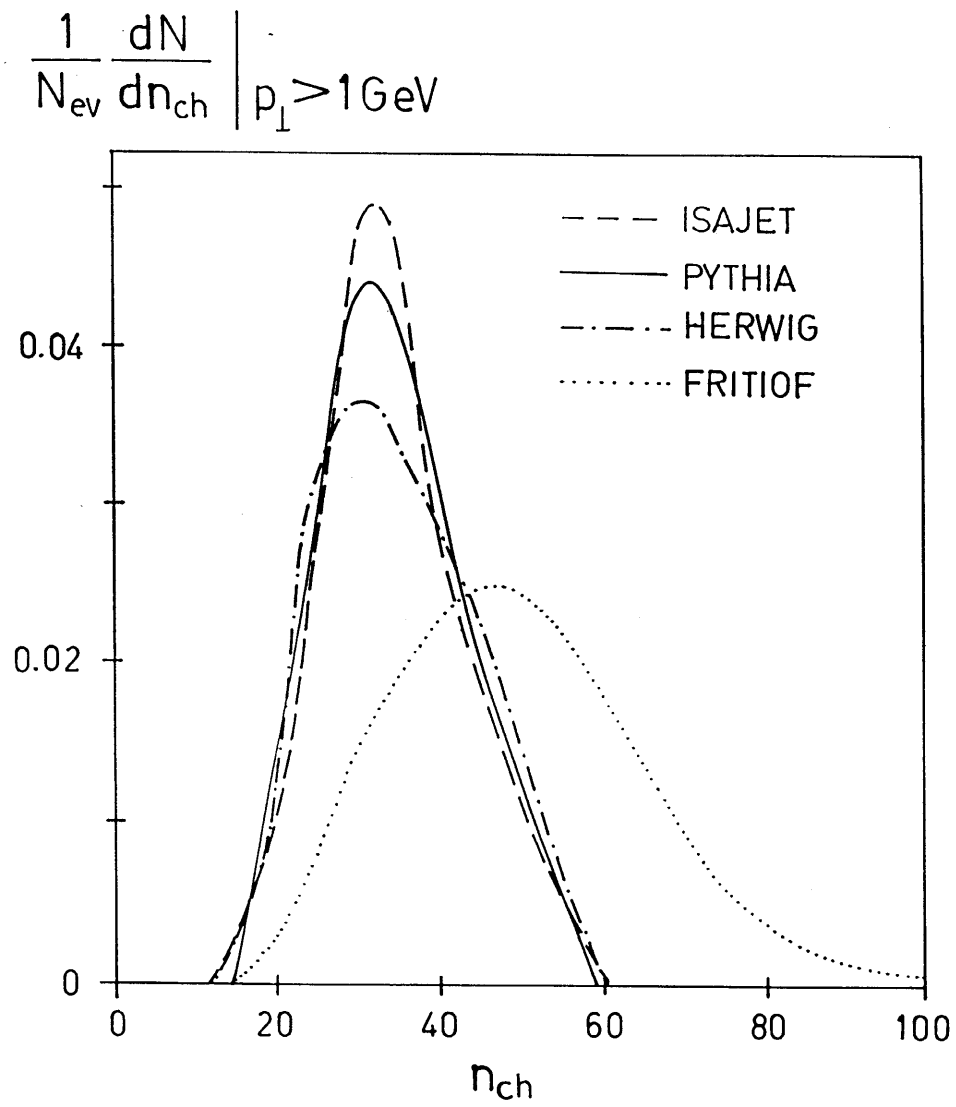
$\frac{1}{N_{ev}} \frac{dN}{dn_{ch}} \Big|_{p_\perp > 1 GeV}$
ISAJET
PYTHIA
HERWIG
FRITIOF
0.04
0.02
0
0
20
40
60
80
100
n_{ch}

Fig. 9b

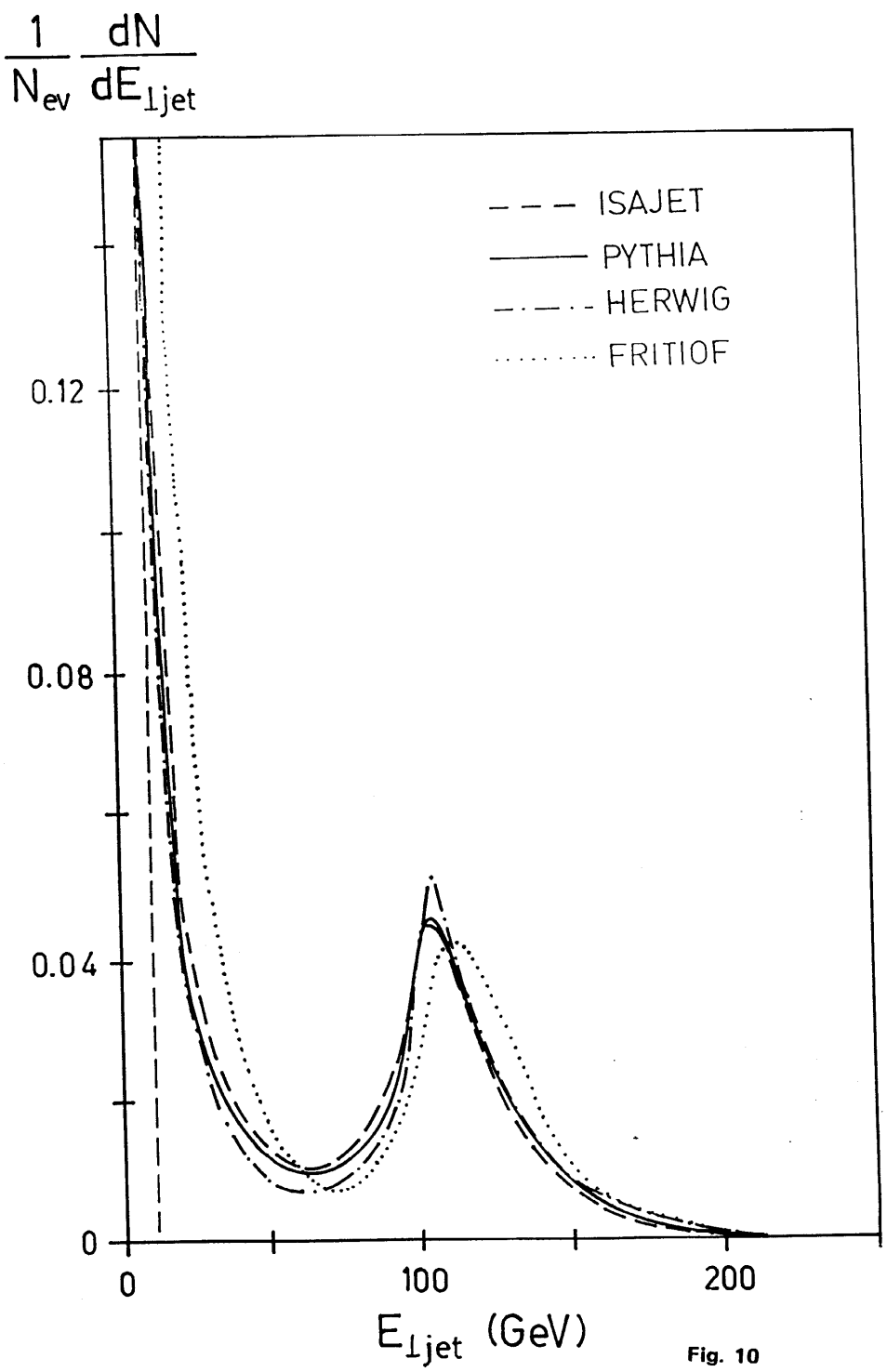
$\frac{1}{N_{ev}} \frac{dN}{dE_{\perp jet}}$
ISAJET
PYTHIA
HERWIG
FRITIOF
0.12
0.08
0.04
0
0
100
200
$E_{\perp jet}$ (GeV)

Fig. 10

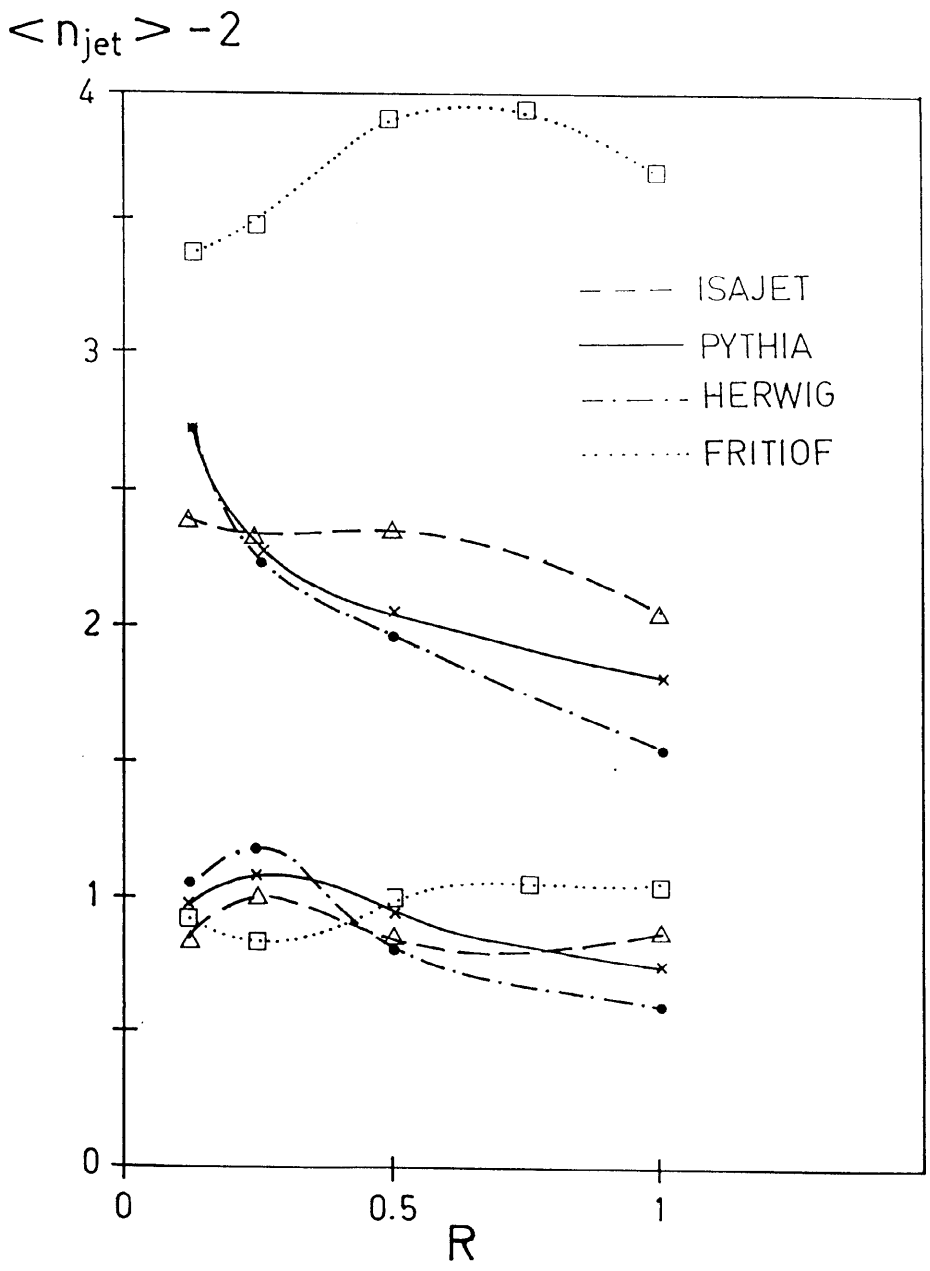
$\langle n_{jet} \rangle - 2$
ISAJET
PYTHIA
HERWIG
FRITIOF
4
3
2
1
0
0
0.5
1
R

Fig. 11

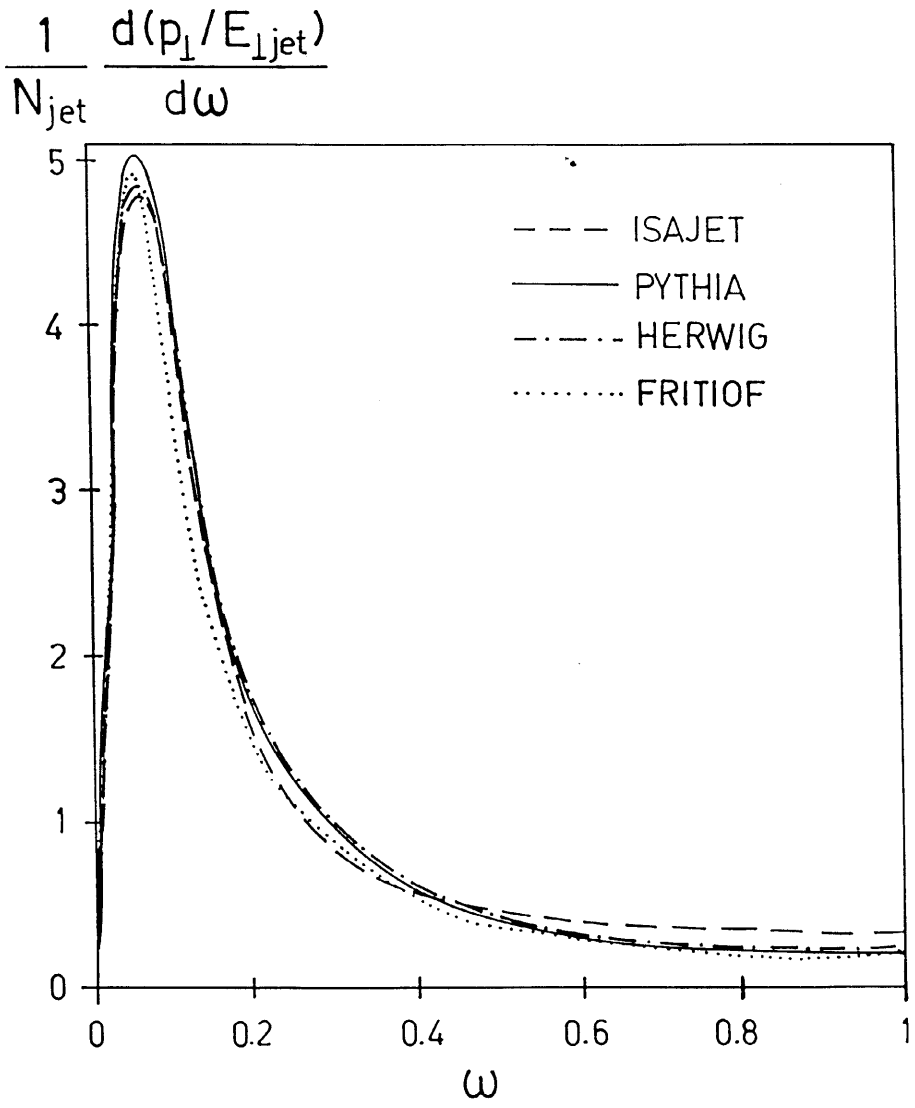
$\frac{1}{N_{jet}} \frac{d(p_\perp / E_{\perp jet})}{d\omega}$
ISAJET
PYTHIA
HERWIG
FRITIOF
0
1
2
3
4
5
0
0.2
0.4
0.6
0.8
1
ω

Fig. 12

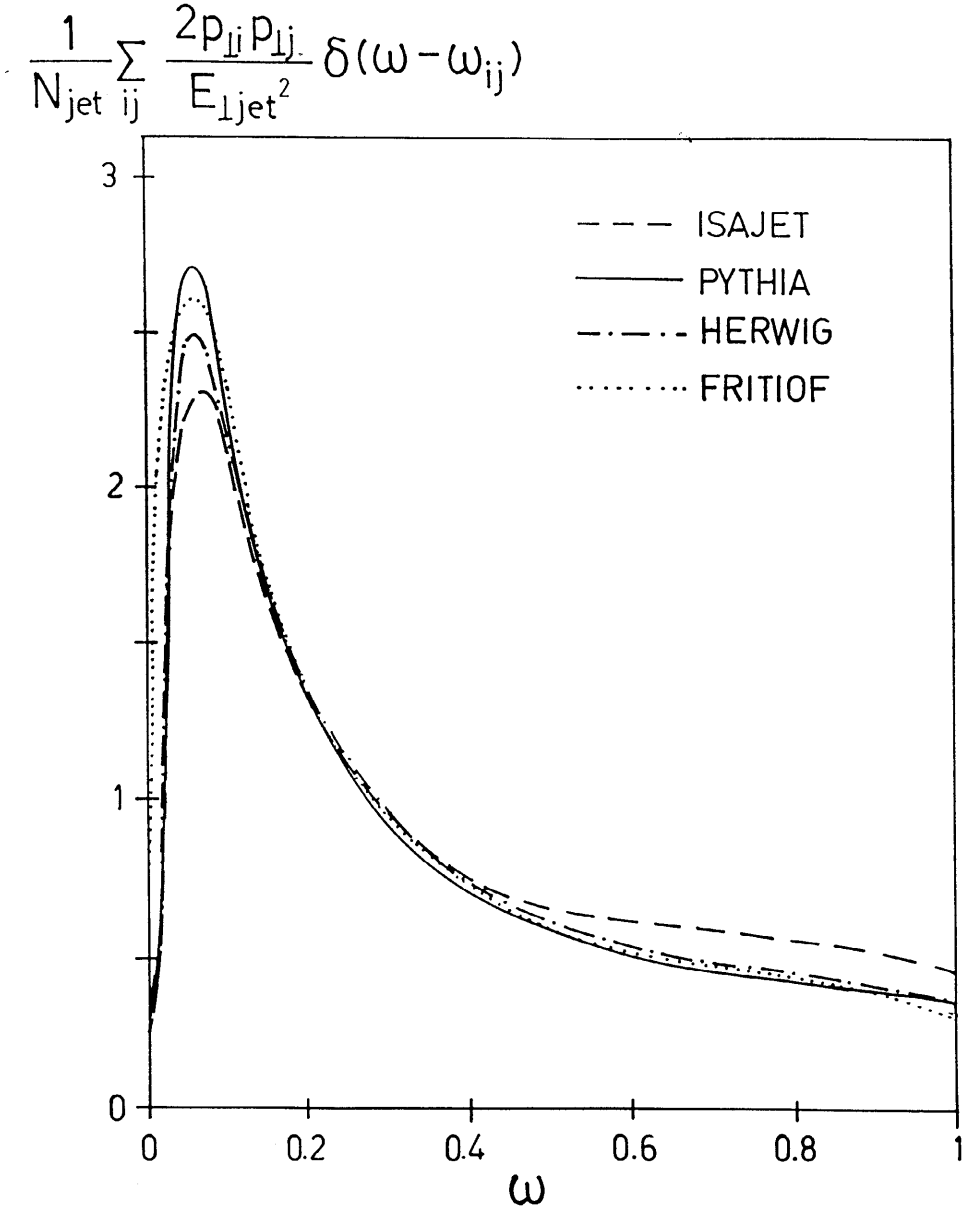
$\frac{1}{N_{jet}} \sum_{ij} \frac{2 p_{\perp i} p_{\perp j}}{E_{\perp jet}^2} \delta(\omega - \omega_{ij})$
ISAJET
PYTHIA
HERWIG
FRITIOF
0
1
2
3
0
0.2
0.4
0.6
0.8
1
ω

Fig. 13

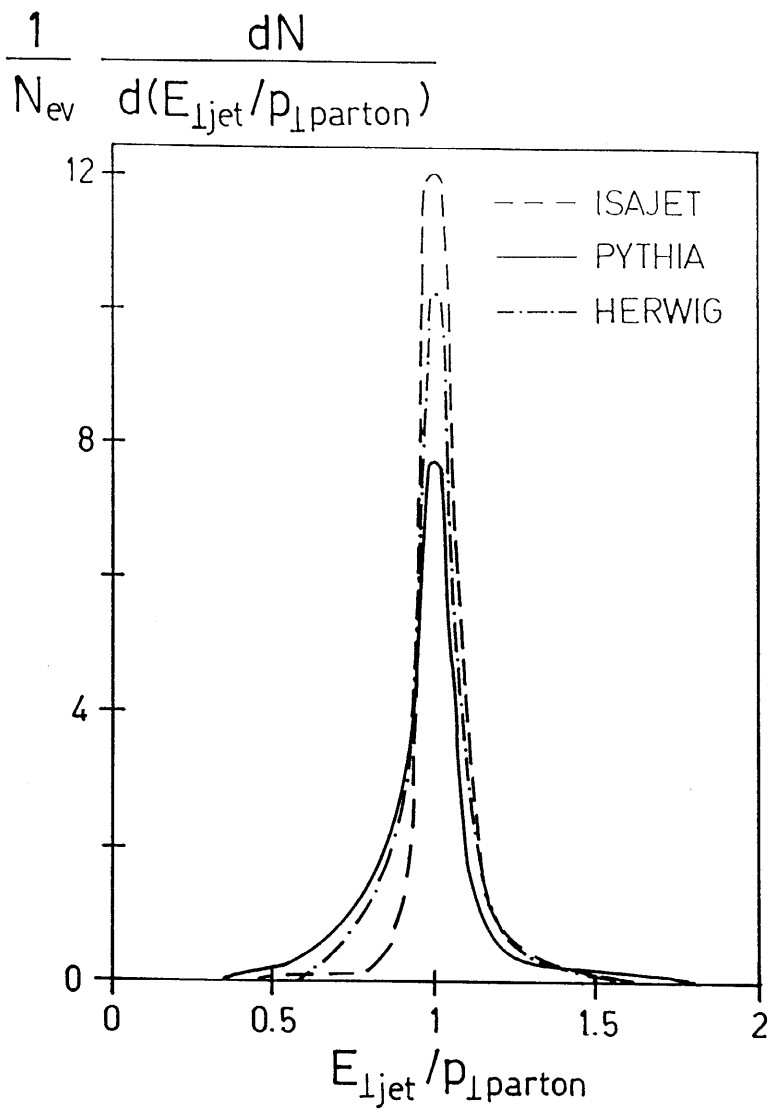
$\frac{1}{N_{ev}} \frac{dN}{d(E_{\perp jet}/p_{\perp parton})}$
12
8
4
0
0
0.5
1
1.5
2
$E_{\perp jet}/p_{\perp parton}$
ISAJET
PYTHIA
HERWIG

Fig. 14

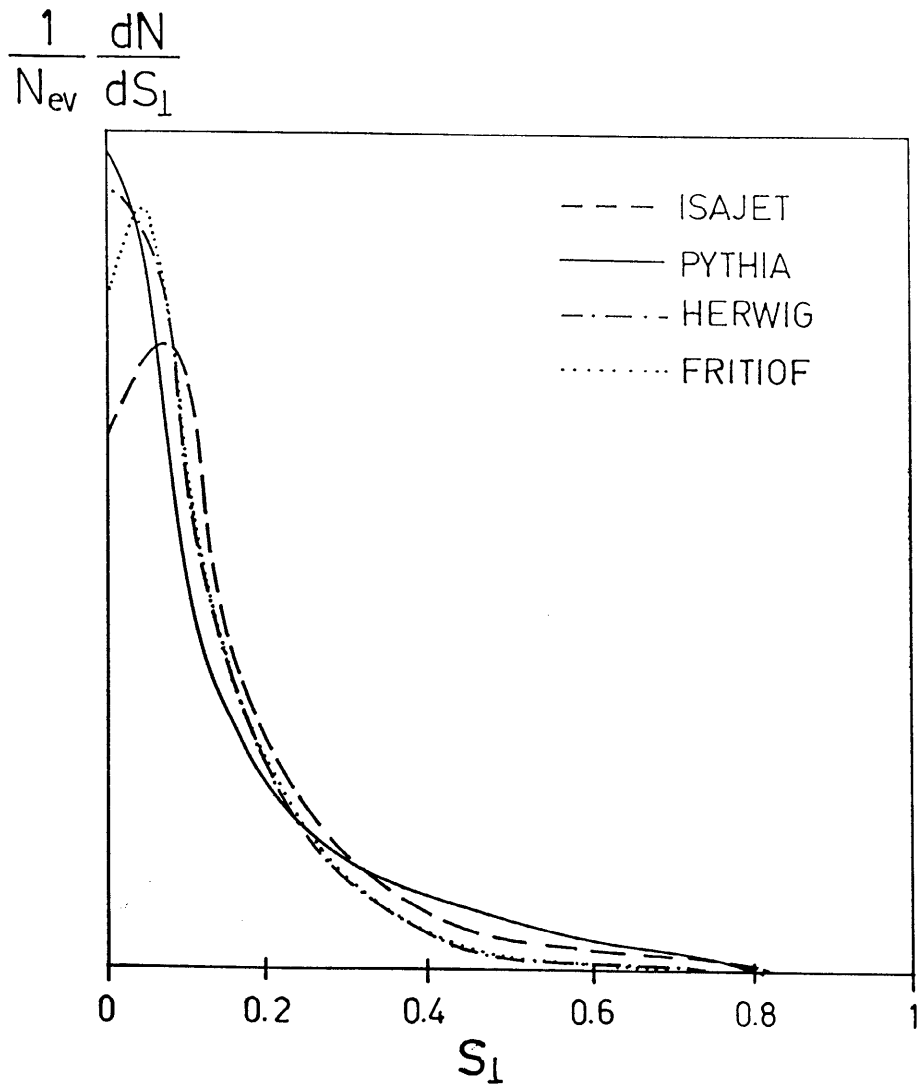
$\frac{1}{N_{ev}} \frac{dN}{dS_\perp}$
0
0.2
0.4
0.6
0.8
1
$S_\perp$
ISAJET
PYTHIA
HERWIG
FRITIOF

Fig. 15

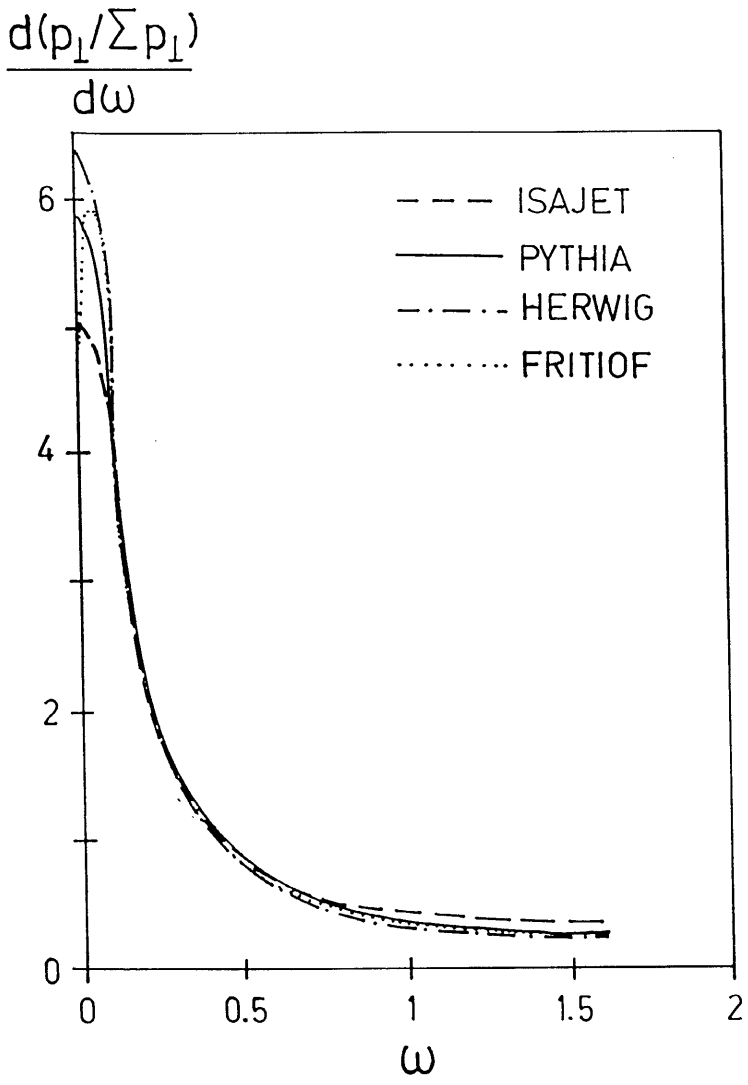
d(p⊥/Σp⊥)
dω
ISAJET
PYTHIA
HERWIG
FRITIOF
0
2
4
6
0
0.5
1
1.5
2
ω

Fig. 16

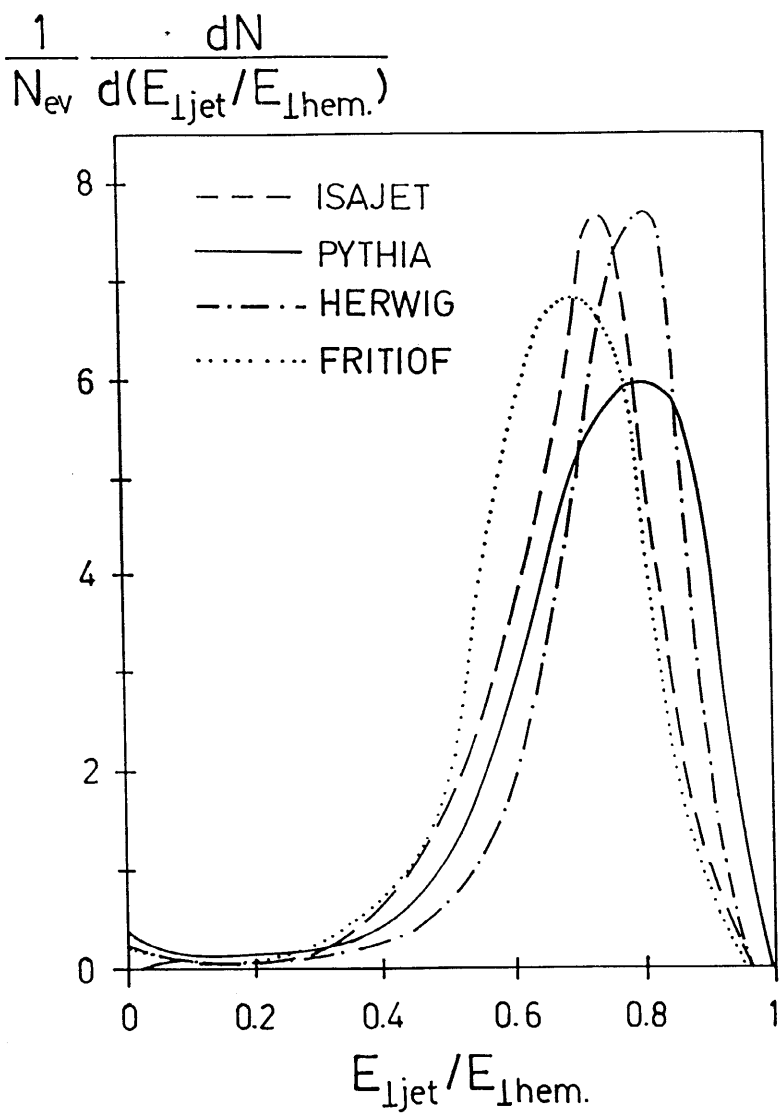
1/N_ev · dN/d(E⊥jet/E⊥hem.)
ISAJET
PYTHIA
HERWIG
FRITIOF
0
2
4
6
8
0
0.2
0.4
0.6
0.8
1
E⊥jet/E⊥hem.

Fig. 17

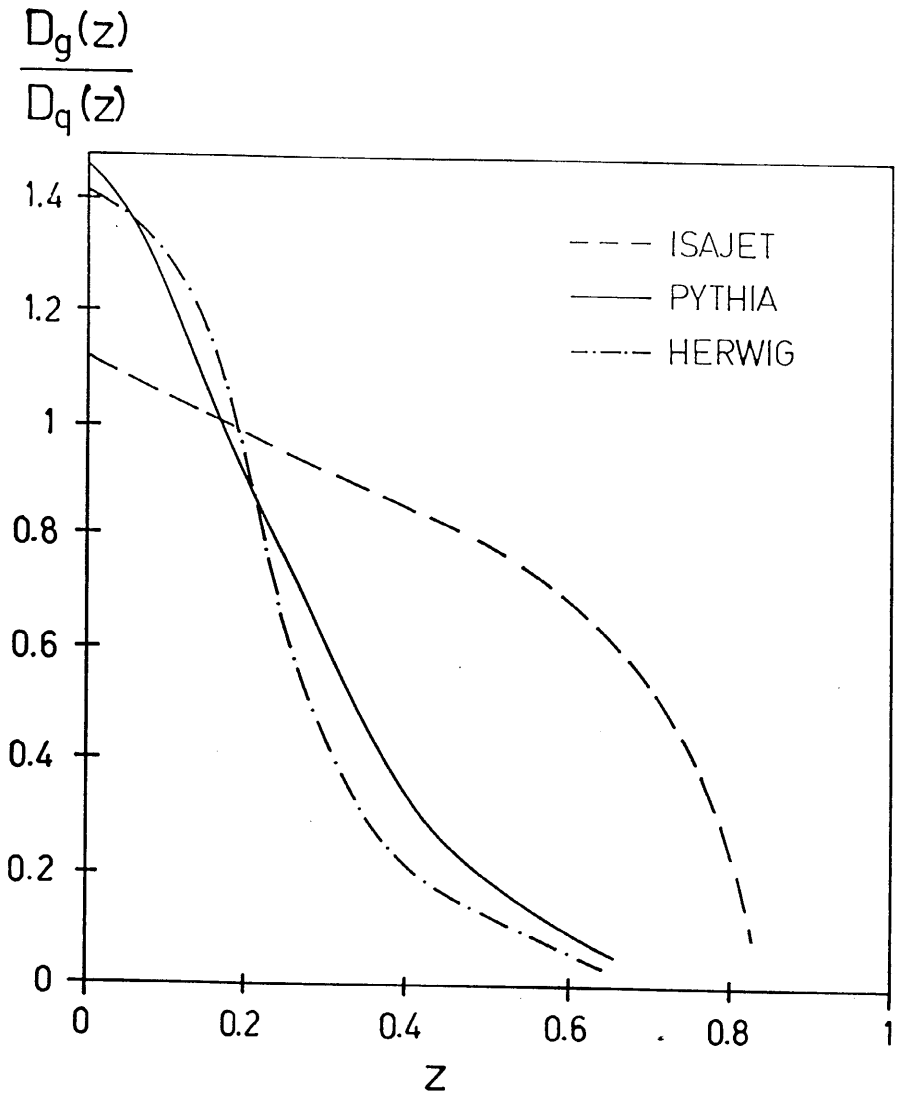

Fig. 18a

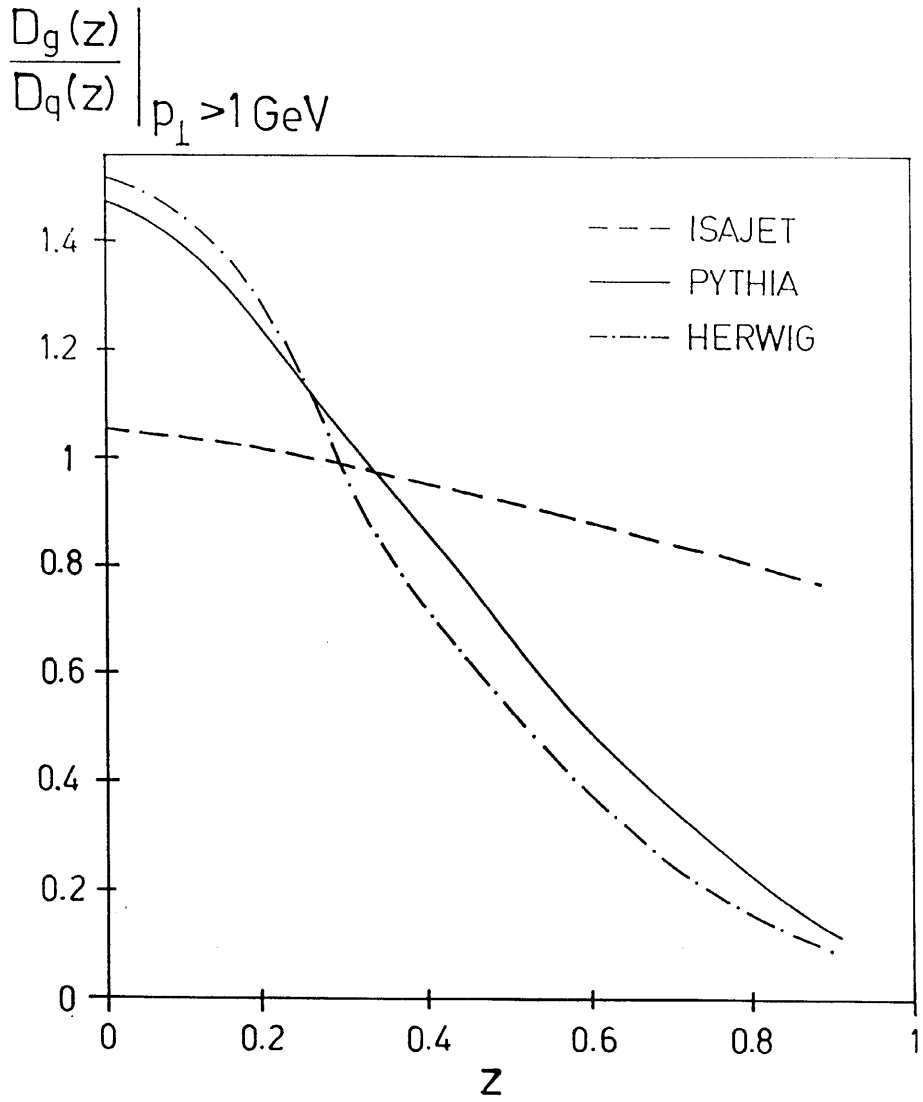

Fig. 18b

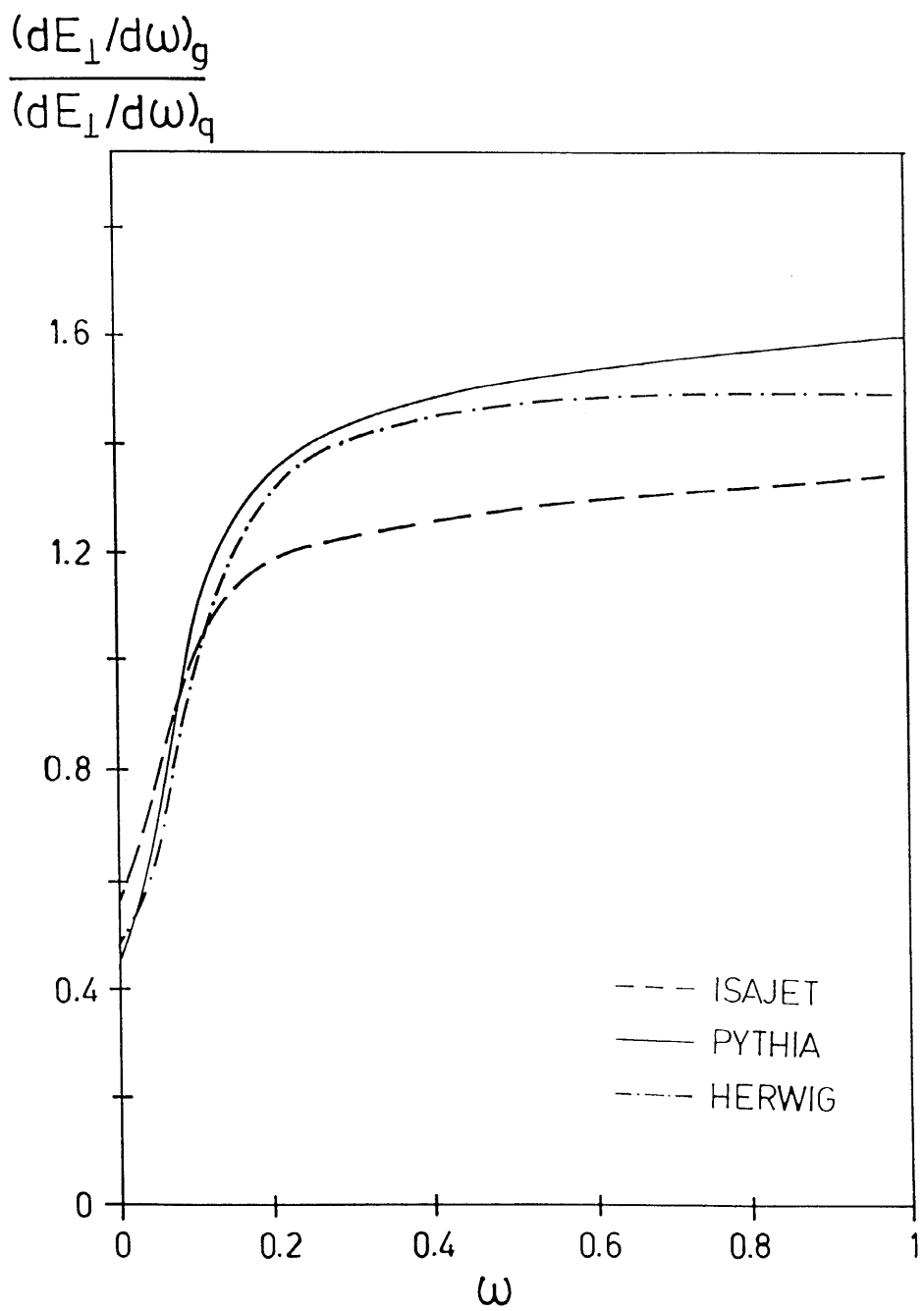
$\frac{(dE_\perp/d\omega)_g}{(dE_\perp/d\omega)_q}$
1.6
1.2
0.8
0.4
0
0
0.2
0.4
0.6
0.8
1
ω
ISAJET
PYTHIA
HERWIG

Fig. 19

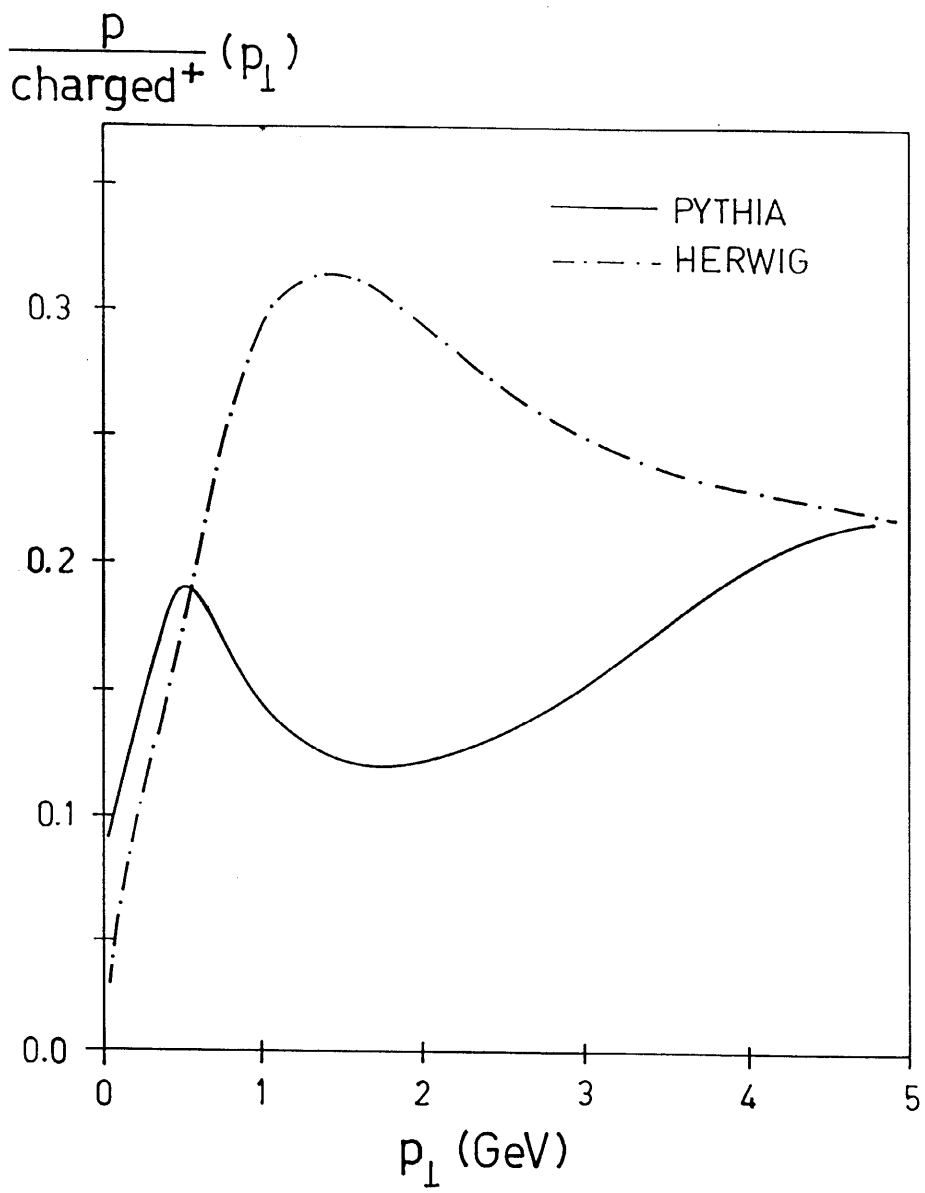
$\frac{p}{charged^+}(p_\perp)$
0.3
0.2
0.1
0.0
0
1
2
3
4
5
$p_\perp$ (GeV)
PYTHIA
HERWIG

Fig. 20